Three loop effective potential for $\langle \frac{1}{2} A_\mu^{a2} \rangle$ in the Landau gauge in QCD

J. A. Gracey

Theoretical Physics Division, Department of Mathematical Sciences, University of Liverpool, P.O. Box 147, Liverpool, L69 3BX, United Kingdom

(Received 25 July 2022; accepted 24 August 2022; published 9 September 2022)

We apply the local composite operator method to construct the three loop effective potential for the dimension two operator $\frac{1}{2} A_\mu^{a2}$ in the Landau gauge in quantum chromodynamics. For $SU(3)$ we show that the three loop value of the effective mass of the gluon is similar to the two loop estimates when the number of massless quarks is strictly less than five for $SU(3)$.

DOI: 10.1103/PhysRevD.106.065006

I. INTRODUCTION

In the last quarter century it has become accepted that the behavior of the Landau gauge gluon propagator in quantum chromodynamics (QCD), as computed on the lattice, is not of the fundamental form [1–9]. In other words it differs from that of the photon in quantum electrodynamics which has a massless pole with respect to the momentum. Instead the gluon propagator is bounded with no singularity at any momentum and moreover freezes to a nonzero value. In the high energy limit, if p is the momentum, then the propagator has a $1/p^2$ asymptotic behavior which is consistent with the Lagrangian construction that gluons behave as effectively free particles analogous to a non-Abelian massless photon. That the gluon propagator freezes at zero momentum indicates that some nonzero mass scale is associated with the infrared properties of the field. This is loosely termed a gluon mass but not because one can identify an isolated state with a massive *fundamental* field. Clearly the presence of such a mass scale, as opposed to a canonical mass, requires further understanding from a theoretical point of view. There has been substantial progress to this end since the early lattice observations of [1] and subsequent confirmations. See, for example, [2–9]. One prior idea centered on Gribov's observation [10] that to globally uniquely fix a covariant gauge in a non-Abelian gauge theory such as QCD requires a restriction on the path integral [10]. In the Landau gauge this introduces a mass scale, the Gribov mass, that satisfies a gap equation equating it to a nonperturbative function of the coupling constant. The fundamental structure of the gluon propagator is modified as well. At large momenta it behaves like the propagator of a massless field with a $1/p^2$ asymptote. By contrast at low momenta the nonzero Gribov mass modifies the propagator in that it is bounded with no singularity and vanishes at zero momenta. Evidently this is out of line with the low momenta lattice results. Several modifications to Gribov's construction have been introduced such as Zwanziger's program to localize the Gribov operator to produce a local renormalizable Lagrangian [11–21] that involves additional spin-1 ghost fields. While this maintained the suppressed gluon propagator in the infrared it was the foundation for a subsequent extension. A dimension two gluon mass operator was also included and studied at length in [22–24]. The localized Gribov-Zwanziger Lagrangian with the extra operator is also renormalizable. In this particular modification of the Gribov construction various composite operators of the fields can develop nonzero vacuum expectation values. Consequently for certain configurations the resulting gluon propagator was much more in line with lattice data in that they froze to a nonzero finite value.

The idea of treating the QCD Lagrangian by appending a simple gluon mass operator without spontaneous symmetry breaking predates Gribov's seminal work. In the mid-1970s Curci and Ferrari [25] investigated a nonlinear gauge fixing of Yang-Mills theory where a Becchi-Rouet-Stora-Tyutin (BRST) invariant dimension two gluon and ghost mass operator was included. This idea fell out of fashion for a while due to the loss of nilpotency of the BRST charge [26–34]. More recently there has been a revival of interest in the model and a gluon mass term. For instance, it was shown in [35–39] that one could connect the mass parameter of the gluon with Gribov copies that arise in the global gauge fixing [10]. In other words one can interpret the mass as an extra gauge parameter reflecting the effect of the copies so that the infrared properties of Yang-Mills theory could be described by a Lagrangian with a gluon mass term. This perspective was tested out at one loop in [37,40,41] where the gluon mass model was used to calculate the gluon propagator analytically and then fitted

to lattice data. There was a reasonable quantitative agreement over virtually all momenta. The inclusion of the two loop corrections was carried out in [42] with a perceptible improvement on the one loop fit over all momenta. This lends support to the idea that a massive gluon could be a useful tool to model infrared phenomena in QCD. One observation was that the mass was of the order of 350 MeV. This was not inconsistent with recent estimates of the mass gap such as fitting models of the gluon propagator to lattice data [43] or via functional renormalization group ideas [44]. Indeed the former article also suggested that a running gluon mass might be sufficient to circumvent the problem of Gribov copies. That such a consistent mass scale emerges in Yang-Mills theory or QCD from different techniques provides evidence that this is a particular infrared property.

While a two loop analysis was carried out in [42] if it is accepted that there is a gluon mass scale then the various Lagrangian field theory approaches ought to be refined by extending them to three loops. However computing the three loop corrections to the gluon propagator in a model with a massive gluon over all momenta along the lines of [42] is not currently possible on technical grounds. For instance, the three loop massive 2-point master Feynman integrals are not available analytically for all momenta. Their values are necessary for the final stage in applying the Laporta algorithm [45], which is the main program for evaluating the various 2-point functions. Instead, as an alternative approach to gain three loop insight, it is possible to study the effect of three loop corrections on the gluon mass gap by another technique. In [46] a method was developed and subsequently refined [47] to compute the effective action and associated effective potential of dimension two operators in a quantum field theory. Termed the local composite operator (LCO) method it was used at one and two loops in [46,47] to study the $SU(N)$ Gross-Neveu model [48]. Although this is a two dimensional renormalizable theory it shares various properties with QCD that include asymptotic freedom, dynamical mass generation and the existence of a mass gap [48]. In the Gross-Neveu model the latter has a significant property in that the N dependence of the mass gap is known *exactly* [49,50], providing a way to benchmark the LCO method. Indeed the mass estimates determined in [46,47] were in close agreement with the exact mass gap expression for a large range of N. Buoyed by this observation the LCO method was applied to Yang-Mills theory at two loops in [51] and later to QCD [52] at the same order. The gluon mass estimates given in [51,52] were roughly $2\Lambda_{\overline{\rm MS}}$ where the definition of the effective mass was the vacuum expectation value of the scalar color singlet field that arises as part of the LCO formalism. As the mass gap value of [51,52] in the early 2000s predated more recent estimates it was difficult then to assess its consistency with other approaches.

Given the recent interest in gluon mass determinations from the lattice, functional renormalization group method, and other approaches such as the Schwinger-Dyson technique, it is the purpose of this article to extend the LCO analysis of Yang-Mills theory and QCD to three loops. To be able to go to this loop order has become possible now with advances in techniques to evaluate high order Feynman integrals. For instance, we will make use of the FORCER algorithm [53,54] as well as the Laporta algorithm [45] to respectively evaluate the four and three loop Feynman integrals that are necessary to construct the three loop effective potential of the dimension two gluon mass operator or equivalently the color singlet scalar that condenses to produce the gluon effective mass. The advantage of the LCO method is that it provides a quantum field theoretic foundation. By this we mean that the effective potential satisfies a homogeneous renormalization group equation and the effective action is linear in the source field associated with the color singlet scalar [46,47,51]. This leads to an effective potential with a well-established energy interpretation [46,47,51] that means a well-defined mass can be extracted from the absolute minimum of the potential which is not the perturbative one. Moreover the underlying Lagrangian, which is modified by the presence of the color singlet scalar, is renormalizable. Once the effective potential has been computed at three loops for an arbitrary color group, we will extract estimates for the effective gluon mass. The definition of the mass we propose to use here will differ from that of the earlier studies of [51,52] which simply involved the vacuum expectation value of the scalar field. Instead we will define the mass as the coefficient of the gluon mass operator in the LCO derived Lagrangian in the nonperturbative vacuum. It will turn out that mass gap estimates derived with this definition will be more stable with respect to loop corrections as well as more in keeping with values deduced by other methods.

The article is organized as follows. We recall the formal aspects of the LCO method in Sec. II in the Yang-Mills theory context including the derivation of the modified Lagrangian. Section III is devoted to the computation of the three loop effective potential that includes the calculation of the underlying fundamental LCO parameter from the evaluation of a four loop massless 2-point function. Aspects of the renormalization of the LCO Lagrangian are also discussed in Sec. III. The three loop effective potential is analyzed in Sec. IV for both $SU(2)$ and $SU(3)$ for a range of quark flavors which lead to estimates of the effective gluon mass. Concluding remarks are provided in Sec. V with an Appendix recording expressions for all the relevant perturbative quantities needed to determine the potential, as well as the potential itself, for a general color group.

II. FORMALISM

We devote this section to reviewing the basics of the LCO method as applied to QCD [51,52] in the Landau

gauge. By way of introducing conventions we recall the QCD Lagrangian is

$$L_{\rm o} = -\frac{1}{4}G^a_{{\rm o}\mu\nu}G^{a\mu\nu}_{\rm o} - \frac{1}{2\alpha_{\rm o}}(\partial^\mu A^a_{{\rm o}\mu})^2 - \bar{c}^a_{\rm o}\partial^\mu D_{{\rm o}\mu}c^a_{\rm o} + i\bar{\psi}^{iI}_{\rm o}\not{D}_{\rm o}\psi^{iI}_{\rm o} \tag{2.1}$$

where the index ranges are $1 \le i \le N_f$, $1 \le a \le N_A$, and $1 \le I \le N_c$, N_f is the number of massless quarks, N_A is the dimension of the adjoint representation, and N_c is the number of colors or equally the dimension of the fundamental representation. All entities in (2.1) are bare as denoted by the subscript $_{\rm o}$. The field strength and covariant derivatives are

$$\begin{aligned} G^a_{\mu\nu} &= \partial_\mu A^a_\nu - \partial_\nu A^a_\mu - g f^{abc} A^b_\mu A^c_\nu \\ D_\mu c^a &= \partial_\mu c^a - g f^{abc} A^b_\mu c^c, \\ D_\mu \psi^{iI} &= \partial_\mu \psi^{iI} + i g T^a_{IJ} A^a_\mu \psi^{iJ} \end{aligned} \tag{2.2}$$

where g is the gauge coupling constant. Although we have included the gauge parameter α in (2.1) it will henceforth be set to the Landau gauge value of zero in all subsequent calculations. We focus on this particular gauge since it is the one that has been most widely studied over many years, using lattice field theory and Schwinger-Dyson methods, meaning that the gluon mass has been estimated in it more than any other gauge. Having recalled the core QCD Lagrangian we now focus on the incorporation of the dimension 2 operator $\mathcal{O} = \frac{1}{2}A^{a2}_\mu$ into the LCO formalism. This is achieved by considering the path integral where the operator is included with a source J leading to the additional term $J\mathcal{O}$ in the Lagrangian which will then have an associated path integral generating functional $W[J]$. Therefore the starting point to treat $\mathcal{O}$ in the LCO method is given by the functional [51]

$$e^{-W[J_{\rm o}]} = \int \mathcal{D}A^\mu_{\rm o}\mathcal{D}\psi_{\rm o}\mathcal{D}\bar{\psi}_{\rm o}\mathcal{D}c_{\rm o}\mathcal{D}\bar{c}_{\rm o} \times \exp\left[\int d^dx\left(L_{\rm o} - \frac{1}{2}J_{\rm o}A^{a2}_{{\rm o}\mu} + \frac{1}{2}\zeta_{\rm o}J^2_{\rm o}\right)\right] \tag{2.3}$$

where everything is expressed in terms of bare quantities. In addition to the linear source term there is a quadratic one. This is necessary to ensure renormalizability which can be seen in several ways. The simplest is through dimensional analysis [51,52]. As the gluon field has dimension 1 then J has dimension 2 and therefore a quadratic term in J is necessary in four dimensions. If such a term was not present then the correlation function of J, which is clearly divergent, would not have an available counterterm to allow the consistent redefinition of the bare Lagrangian in terms of renormalized variables. Separately the additional parameter ζ has been introduced in order to ensure that the renormalization group equation for $W[J]$ is homogeneous [46,47,51]. The actual form of the renormalized parameter will be calculated later via the renormalization group construction and will be a perturbative function of the coupling constant [46,47,51].

As the bare Lagrangian $L_{\rm o}$ has already been given, the renormalized quantities are defined in the canonical way by

$$\begin{aligned} &A^a_{{\rm o}\mu} = \sqrt{Z_A}A^a_\mu, \qquad \bar{c}^a_{\rm o} = \sqrt{Z_c}c^a, \qquad \psi^{iI}_{\rm o} = \sqrt{Z_\psi}\psi^{iI}, \\ &g_{\rm o} = \mu^\epsilon Z_g g, \qquad \alpha_{\rm o} = \frac{Z_A}{Z_\alpha}\alpha \end{aligned} \tag{2.4}$$

where μ is the scale introduced to ensure the coupling constant remains dimensionless in dimensional regularization in $d = 4 - 2\epsilon$, which we use throughout, and the source renormalization is achieved via [46,47,51]

$$J_{\rm o} = \frac{Z_m}{Z_A}J, \qquad \zeta_{\rm o}J^2_{\rm o} = (\zeta + \delta\zeta)J^2. \tag{2.5}$$

The quantity $\delta\zeta$ should be regarded as a counterterm and Z_m is the renormalization constant associated with the renormalization of the dimension two operator $\mathcal{O}$ or equivalently the gluon mass. Consequently we have

$$e^{-W[J]} = \int \mathcal{D}A_\mu\mathcal{D}\psi\mathcal{D}\bar{\psi}\mathcal{D}c\mathcal{D}\bar{c} \times \exp\left[\int d^dx\left(L - \frac{1}{2}Z_m J A^{a2}_\mu + \frac{1}{2}(\zeta + \delta\zeta)J^2\right)\right] \tag{2.6}$$

for the generating functional for J in terms of renormalized quantities.

Next we recall the procedure to find ζ as an explicit function [46,47,51]. This will be achieved from the renormalization group properties of $W[J]$ which imply

$$\left[\mu\frac{\partial}{\partial\mu} + \beta(a)\frac{\partial}{\partial a} - \gamma_m(a)\int_x J\frac{\delta}{\delta J} + \mu\frac{\partial\zeta}{\partial\mu}\frac{\partial}{\partial\zeta}\right]W[J] = 0 \tag{2.7}$$

where we have set $a = g^2/(16\pi^2)$. From (2.5) we can deduce that

$$\mu\frac{\partial\zeta}{\partial\mu} = 2\gamma_m(a)\zeta + \delta(a) \tag{2.8}$$

where $\delta(a)$ is in effect the anomalous dimension of J and is determined from the counterterm via [46,47,51]

$$\delta(a) = \left[2\epsilon + 2\gamma_m(a) - \beta(a)\frac{\partial}{\partial a}\right]\delta\zeta \tag{2.9}$$

in order for $W[J]$ to satisfy a homogeneous renormalization group equation [46,47,51]. As it stands presently this

renormalization group function follows from the standard procedure for treating bare parameters in a renormalizable theory. In the context of the LCO method the origin of the $\delta\zeta$ counterterm is due to the requirement of the quadratic term in J for renormalizability since the 2-point correlation function of J is divergent. This implies that $W[J]$ is not linear in the source which would rule out an energy interpretation for the action after a Legendre transformation. Equally the parameter ζ is undetermined at this point. To resolve this [46,47,51], ζ is chosen to be the solution of the first order differential equation

$$\beta(a)\frac{\partial\zeta(a)}{\partial a} = 2\gamma_m(a)\zeta(a) + \delta(a). \tag{2.10}$$

In other words the running of $\zeta(a)$ is determined from that of the coupling constant. If one examines the a dependence of the various known expressions in (2.10) we note that $\beta(a) = O(a^2)$, $\gamma_m(a) = O(a)$ and $\delta(a) = O(1)$ implying the leading term of $\zeta(a)$ has to be $O(1/a)$. Therefore one formally solves (2.10) perturbatively using the ansatz

$$\zeta(a) = \sum_{n=-1}^{\infty} c_n a^n \tag{2.11}$$

which produces a *unique* function of the coupling constant leading to the homogeneous renormalization group equation for $W[J]$ [46,47,51],

$$\left[\mu\frac{\partial}{\partial\mu} + \beta(a)\frac{\partial}{\partial a} - \gamma_m(a)\int_x J\frac{\delta}{\delta J}\right]W[J] = 0. \tag{2.12}$$

The main consequence of this is that Δ, given by

$$\Delta = \frac{\delta W[J]}{\delta J}, \tag{2.13}$$

has a well-defined vacuum expectation value and its effective action follows from

$$\Gamma[\Delta] = W[J] - \int_x J\Delta. \tag{2.14}$$

Consequently the effective action satisfies

$$\left[\mu\frac{\partial}{\partial\mu} + \beta(a)\frac{\partial}{\partial a} + \gamma_m(a)\int_x \Delta\frac{\delta}{\delta\Delta}\right]\Gamma[\Delta] = 0 \tag{2.15}$$

which is the standard formal renormalization group equation.

In order to determine the effective action and thereby the effective potential we need to compute $W[J]$ and execute the inversion (2.14). For the case when $W[J]$ is linear in J this is straightforward but for the present case the dependence on J is quadratic. The LCO method bypasses this difficulty for $\mathcal{O}$ by introducing a Hubbard-Stratonovich transformation that introduces a purely scalar color singlet field σ. Within the path integral this is effected by including unity in a redundant way [46,47,51] via

$$1 = \int \mathcal{D}\sigma \exp\left(-[b_1\sigma + b_2 A_\mu^{a2} + b_3 J]^2\right). \tag{2.16}$$

The free parameters b_i are chosen in such a way as to cancel off the quadratic term in J^2 and the interaction of J with the gluon. In the exponent of the integrand in (2.16) there will be six terms but two of these will be cancelled by choices of b_2 and b_3 leaving four terms. One of these terms will be linear in J and σ allowing b_1 to be fixed so that the new expression for $W[J]$ takes the form

$$e^{-W[J]} = \int \mathcal{D}A_\mu \mathcal{D}\psi\mathcal{D}\bar{\psi}\mathcal{D}c\mathcal{D}\bar{c}\mathcal{D}\sigma \exp\left[\int d^dx\left(L^\sigma - \frac{\sigma J}{g}\right)\right]. \tag{2.17}$$

Each of the remaining three terms of (2.16) will involve only fields and in particular A_μ^a and σ. These are absorbed into a redefinition of the original action to produce the new Lagrangian

$$L^\sigma = L_{\rm o} - \frac{\sigma^2}{2g^2\zeta(a)Z_\zeta} + \frac{Z_m}{2g\zeta(a)Z_\zeta}\sigma A_\mu^a A^{a\mu} - \frac{Z_m^2}{8\zeta(a)Z_\zeta}(A_\mu^a A^{a\mu})^2 \tag{2.18}$$

where

$$Z_\zeta = 1 + \frac{\delta\zeta}{\zeta(a)}. \tag{2.19}$$

The consequence is that with (2.18) one can determine $\Gamma[\Delta]$ using standard techniques of perturbation theory allowing one to deduce the effective potential. The only difference for QCD is that its Feynman rules have to be amended by the additional terms in (2.18) of a modified quartic gluon vertex as a well as a momentum independent propagator for the σ field and its 3-point interaction with the gluon.

III. DETERMINATION OF THE EFFECTIVE POTENTIAL

Having concentrated on the formalism that allows us to extract the effective potential for the Landau gauge gluon mass operator we devote this section to the actual computations that lead to the three loop expression. As is clear from the previous section, various renormalization group functions are required to find $\zeta(a)$ such as $\beta(a)$, $\gamma_m(a)$, and $\delta(a)$. Moreover as explained these are needed at the four loop level. As the QCD Lagrangian has been renormalized to five loops now in the $\overline{\rm MS}$ scheme [55–58], the only

renormalization constants that are needed to extend the two loop effective potential of [51,52] are Z_m and the counterterm for ζ. The former is in fact already available at five loops in the $\overline{\text{MS}}$ scheme in the Landau gauge via a simple Slavnov-Taylor identity. It was shown in [59] originally and subsequently observed in [60] via a three loop calculation that Z_m is not independent but related to Z_A and Z_c in the Landau gauge. This identity was later verified in more detail in [61]. Indeed similar Slavnov-Taylor identities have been constructed for the BRST invariant gluon mass operators in two nonlinear gauges. These are the Curci-Ferrari [25] and maximal Abelian gauges [62–64] with the identities being discussed in [65,66] and [67,68] respectively. So $\gamma_m(a)$ in the Landau gauge can be deduced from the combination $\gamma_A(a) + \gamma_c(a)$.

Therefore it only remains to determine $\delta\zeta$. An efficient method to deduce this was outlined in [52] but followed a different but equivalent strategy to that given in [51]. In [52] the divergence structure of the correlation function of J or equivalently that of $\mathcal{O}$ was considered in the massless theory. This Green's function is indicated graphically in Fig. 1. Unlike say the correlation function of the field strength, all Feynman graphs contributing to this Green's function will only have two gluons emanating from each operator insertion. Strictly the LCO method will produce a nonzero mass for the gluon and therefore one should in principle determine the Green's function with massive gluon propagators. However as only the ultraviolet divergences are required for the counterterm $\delta\zeta$ massless gluon propagators will suffice. The advantage of this, as noted in [52], was that the Green's function could be computed using the automatic Feynman diagram package MINCER [69,70]. In following the same strategy here we use instead the recent extension of that program which is FORCER [53,54]. Both packages determine the divergences of massless 2-point functions as a function of ϵ. The MINCER package was designed for three loop computations but with the current need for more precision in quantum field theory FORCER was developed to calculate four loop graphs. This is a key point since the LCO formalism requires that $\delta\zeta$ has to be calculated to four rather than three loops here. For the two loop effective potential of [51] the three loop term of $\delta\zeta$ was needed which is why MINCER was the appropriate tool. Therefore we have used FORCER to reevaluate and verify the three loop counterterm before extending it to four loops here. As background there are 1, 5, 67, and 1242 Feynman graphs at the respective successive loop orders from one to four. These were generated by the QGRAF package [71], which is the starting point for the automatic computation of the Feynman graphs contributing to the four loop J correlation function. Throughout we employed the symbolic manipulation language FORM [72,73] for handling the tedious amounts of algebra. Indeed the FORCER package is written in FORM. Equally we made use of the FORM based `color.h` module [72] to evaluate the group theory associated with each graph. That routine is based on the comprehensive article [74] on non-Abelian groups.

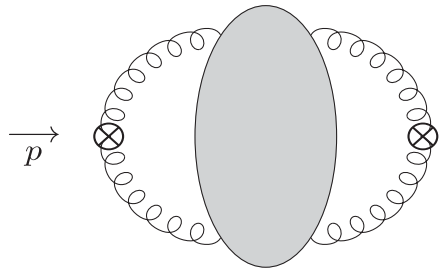

FIG. 1. Correlation function for the operator source J or $\mathcal{O}$ where $\otimes$ denotes the insertion of J or $\mathcal{O}$.

Consequently we have been able to deduce the counterterm $\delta\zeta$ to four loops for an arbitrary color group. As the full expression for it is large it has been provided in the Appendix with electronic versions of all the major expressions computed in this article provided in the associated data file [75]. This means that the various quantities that are derived from $\delta\zeta$ are as large and also recorded in that appendix. However in order to represent the procedure to derive the effective potential we will present the key equations in this section for the case of $SU(3)$ and $N_f = 3$. Therefore the counterterm for the renormalization of J is

$$\begin{aligned}\delta\zeta|^{SU(3)}_{N_f=3} = &-\frac{12}{\epsilon} + 3\left[\frac{27}{\epsilon^2} - \frac{82}{\epsilon}\right]a + \left[-\frac{7290}{\epsilon^3} + \frac{26934}{\epsilon^2} + [1443\zeta_3 - 55109]\frac{1}{\epsilon}\right]\frac{a^2}{12} \\ &+ \left[\frac{5511240}{\epsilon^4} - \frac{24184980}{\epsilon^3} - [801252\zeta_3 + 56625408]\frac{1}{\epsilon^2}\right. \\ &\left. + [15906120\zeta_5 - 1781190\zeta_4 - 1771416\zeta_3 - 109560851]\frac{1}{\epsilon}\right]\frac{a^3}{1152} + O(a^4) \end{aligned} \tag{3.1}$$

where ζ_n is the Riemann zeta function. Converting this to a renormalization group function via (2.9) leads to

$$\begin{aligned}\delta(a)|^{SU(3)}_{N_f=3} = &-24 - 984a + [1443\zeta_3 - 55109]\frac{a^2}{2} + [15906120\zeta_5 - 1781190\zeta_4 - 1771416\zeta_3 - 109560851]\frac{a^3}{144} \\ &+ O(a^4). \end{aligned} \tag{3.2}$$

It is a simple matter now to perturbatively solve the consistency equation that determines $\zeta(a)$ and find

$$\frac{1}{\zeta(a)}\bigg|_{N_f=3}^{SU(3)} = \frac{3}{8}a - \frac{1189}{288}a^2 + [567891\zeta_3 - 2627074]\frac{a^3}{155520} + [72516983400\zeta_5 - 9659825910\zeta_4 - 22815926343\zeta_3 - 80343163558]\frac{a^4}{235146240} + O(a^5). \quad (3.3)$$

The final quantity required prior to computing the effective potential is the renormalization constant

$$Z_\zeta^{-1}|_{N_f=3}^{SU(3)} = 1 + \frac{9a}{2\epsilon} + \left[-\frac{243}{\epsilon^2} + \frac{1025}{\epsilon}\right]\frac{a^2}{24} + \left[\frac{590490}{\epsilon^3} - \frac{1592865}{\epsilon^2} + [6529841 - 16524\zeta_3]\frac{1}{\epsilon}\right]\frac{a^3}{12960} + O(a^4) \quad (3.4)$$

deduced from (3.1) and (3.3) using (2.19).

The foundation has now been put in place from the LCO construction for the effective potential of $\mathcal{O}$ to be determined. By this we mean the renormalization constants of the variables have been found to the necessary order to produce a finite three loop expression. As we will be using (2.17) and (2.18) as the starting point for the process, since for instance there is a linear source term for σ, we follow the standard procedure for deducing an effective potential. At the outset it is worth noting related articles in this area that were useful for this task. These were the three loop effective potentials given in [76] for $O(N)$ ϕ^4 theory, the application of the LCO method to a scalar theory [77], and most usefully the comprehensive study of [78] for a general renormalizable theory that includes the Standard Model. First, to set the scene we recall that the one loop effective potential $V_1(\sigma)$ is deduced from an infinite set of n-point functions with a constant external σ field. Summing this class of functions produces

$$V_1(\sigma) = \frac{\sigma^2}{2g^2\zeta(a)Z_\zeta} + \frac{(d-1)N_A}{2}\int\frac{d^dk}{(2\pi)^d}\ln\left(k^2 + \frac{Z_m\sigma}{gZ_\zeta\zeta(a)}\right) \quad (3.5)$$

where we have included the renormalization constants as these are necessary for the higher order corrections. The factor of $(d-1)$ arises from the contraction of the Lorentz indices of the massive Landau gauge gluon propagator with the mass given by [51,52]

$$m^2 = \frac{Z_m\sigma}{gZ_\zeta\zeta(a)} \quad (3.6)$$

and N_A appears from the trace of the adjoint color indices.

To proceed to the two and three loop corrections one does not have to tediously resum corrections to the leading n-point functions with a constant σ field. Instead one equivalently computes the respective loop order vacuum graphs based on the interactions in L^σ but with a new field $\tilde{\sigma}$. This is introduced by the simple shift [51,52],

$$\sigma = \langle\sigma\rangle + \tilde{\sigma} \quad (3.7)$$

where the expectation value of σ is a constant. We note that the propagator for $\tilde{\sigma}$ derives from the coefficient of $\tilde{\sigma}^2$ in L^σ after applying (3.7). Again we have used QGRAF to generate the two and three loop vacuum graphs. The graphs that contribute at two loops are shown in Fig. 2 where the spring lines are gluons, the dotted directed lines are quarks, the solid directed lines are Faddeev-Popov ghosts, and the double solid lines correspond to $\tilde{\sigma}$. We note that the interactions of the latter involve $\zeta(a)$. At three loops more graphs contribute to the effective potential and these are shown across three figures. The ones based on the benz topology are given in Fig. 3 while those based on the ladder topology are given in Fig. 4. The remaining graphs are provided in Fig. 5 which include the one loop propagator corrections to the two loop graphs of Fig. 2 from massive gluon snail graphs as well as vertex corrections to the same graphs.

The next stage in the process is the evaluation of the 5 two loop and 29 three loop vacuum graphs for $V(\sigma)$. As with the derivation of $\delta\zeta$ at four loops we have carried this out by an automatic Feynman diagram computation. Unlike that case the subsequent integrals are massive since we assume $\langle\sigma\rangle$ is nonzero and therefore we cannot apply the FORCER algorithm. Instead we employ the Laporta algorithm [45] where all the integrals contributing to a vacuum graph are reduced to a small set of core master integrals. In practical terms we used the REDUZE implementation of the algorithm [79] to achieve this. While analytic expressions for three (and higher) loop vacuum master graphs have been determined by various methods we use the results provided in [80] for our automatic computation. This is because [80] gathers and summarizes the earlier work of [81] on the vacuum benz topologies as well as that of others [82–84] with the same conventions. To ensure that the final result is ultimately finite, as the counterterms are already determined, the master two loop master integrals have to be expanded to the requisite order in ϵ. Such terms are available in the expressions recorded in [80]. In addition $V_1(\sigma)$ has to be expanded to $O(\epsilon^2)$ prior to the substitution of the various renormalization constants.

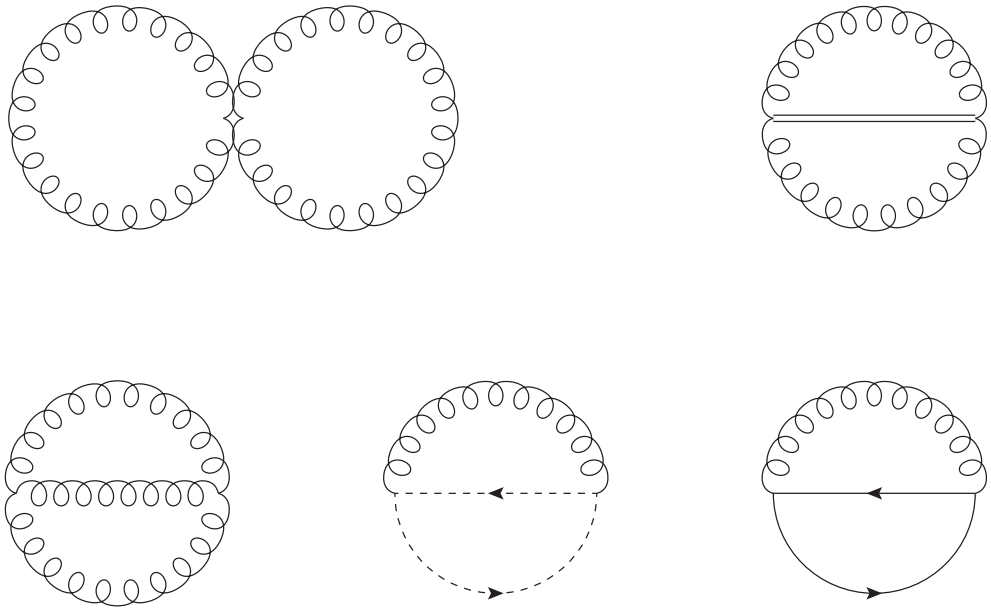

FIG. 2. Two loop graphs contributing to the effective potential.

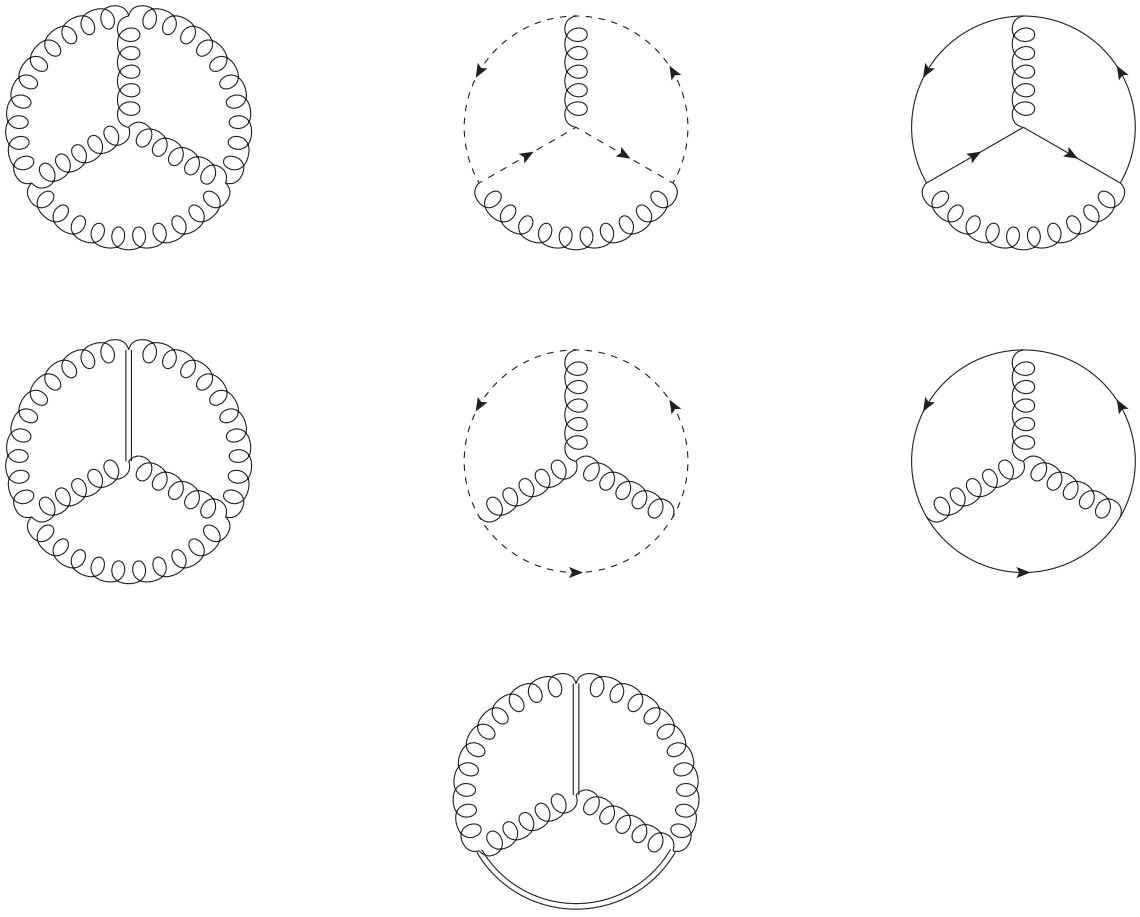

FIG. 3. Three loop benz graphs contributing to the effective potential.

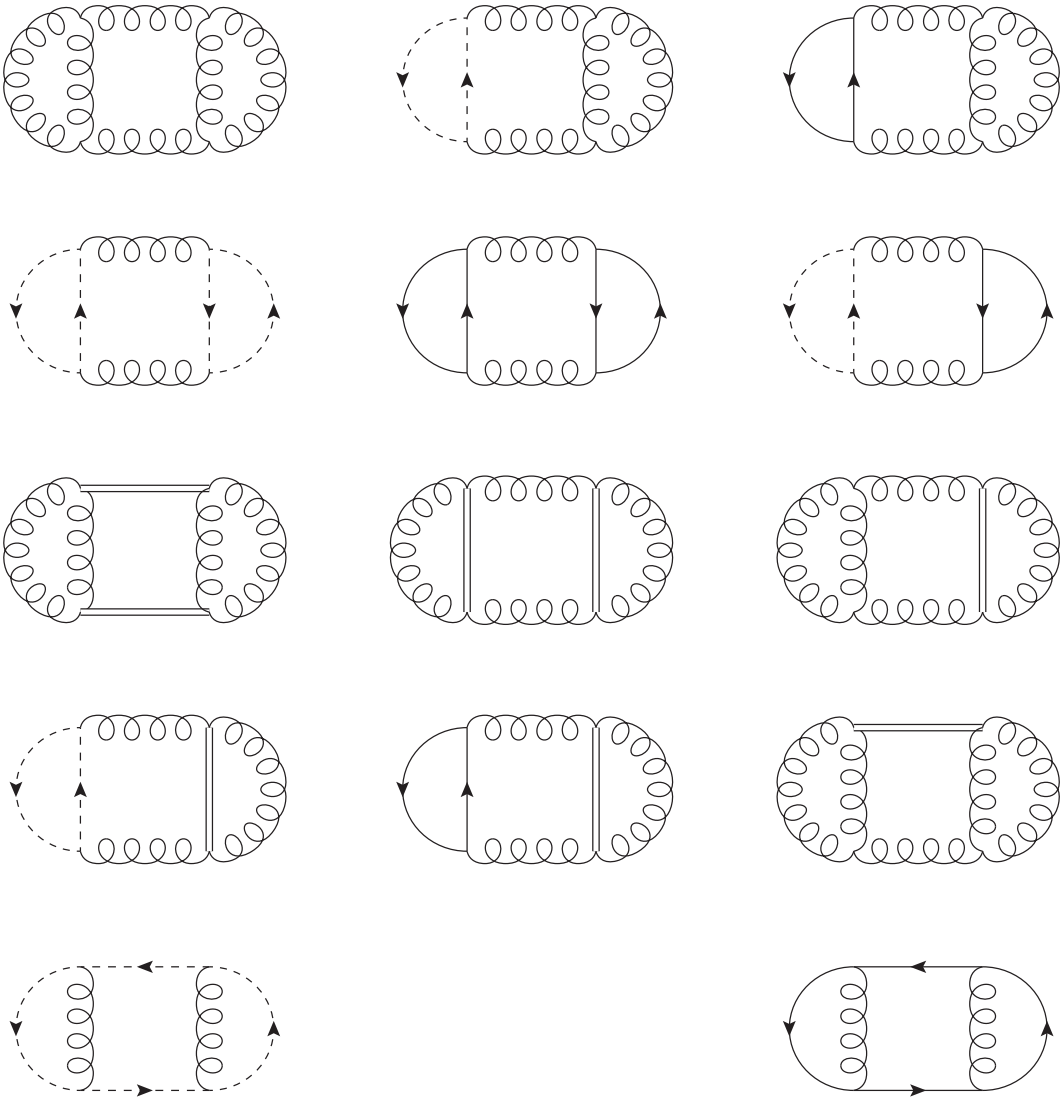

FIG. 4. Three loop ladder graphs contributing to the effective potential.

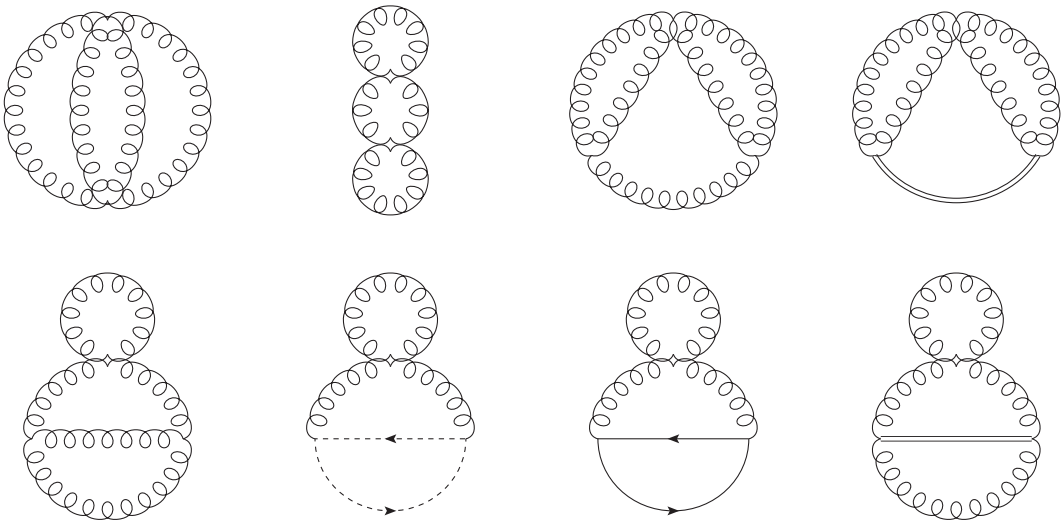

FIG. 5. Remaining three loop graphs contributing to the effective potential.

Collecting the various contributions from the graphs together with the renormalization constants determined to the necessary order we arrive at the three loop effective potential in the $\overline{\text{MS}}$ scheme. As our focus in this section is for $SU(3)$ and $N_f = 3$ we note

$$V(\sigma)|^{SU(3)}_{N_f=3} = \left[\frac{4}{3} + \left[6\overline{\ln}(\bar{g}\bar{\sigma}) - \frac{1594}{81}\right]a + \left[\frac{779}{60}\zeta_3 + \frac{45}{2}\zeta_2 - \frac{3340906}{10935} + \frac{297}{2}\sqrt{3}\text{Ls}_2\left(\frac{2\pi}{3}\right) + \frac{1106}{9}\overline{\ln}(\bar{g}\bar{\sigma}) - \frac{27}{2}\overline{\ln}^2(\bar{g}\bar{\sigma})\right]a^2 + \left[\frac{828955}{756}\zeta_5 + \frac{69153}{64}\zeta_4 + \frac{7742747}{12960}\zeta_3 + \frac{40319}{96}\zeta_2 - \frac{91909989967}{9447840} - 1769\text{Li}_4\left(\frac{1}{2}\right) - \frac{3321}{32}\text{Ls}_2^2\left(\frac{2\pi}{3}\right) + \frac{1769}{4}\ln^2(2)\zeta_2 - \frac{1769}{24}\ln^4(2) + \frac{121}{6}\sqrt{3}\pi^3 + \frac{5659}{4}\sqrt{3}\text{Ls}_2\left(\frac{2\pi}{3}\right) + \left[\frac{1924658}{405} - \frac{2541}{40}\zeta_3 - \frac{6075}{16}\zeta_2 - \frac{8019}{4}\sqrt{3}\text{Ls}_2\left(\frac{2\pi}{3}\right)\right]\overline{\ln}(\bar{g}\bar{\sigma}) - \frac{1767}{2}\overline{\ln}^2(\bar{g}\bar{\sigma}) + \frac{243}{4}\overline{\ln}^3(\bar{g}\bar{\sigma})\right]a^3\Bigg]\bar{\sigma}^2 + O(a^4) \tag{3.8}$$

where $\bar{g} = \frac{g}{4\pi}$, $\text{Li}_n(z)$ is the polylogarithm function,

$$\overline{\ln}(z) = \ln\left(\frac{z}{\mu^2}\right), \tag{3.9}$$

the log-sine function is

$$\text{Ls}_n(\theta) = -\int_0^\theta dz \ln^{n-1}\left|2\sin\left(\frac{1}{2}z\right)\right| \tag{3.10}$$

noting that $\text{Ls}_2(\theta) = \text{Cl}_2(\theta)$ with $\text{Cl}_2(\theta)$ denoting the Clausen function and we have introduced the shorthand notation

$$\sigma = \frac{9N_A}{(13C_A - 8T_F N_f)}\bar{\sigma} \tag{3.11}$$

with the color dependent factor arising from the coefficient of the leading term of $\zeta(a)$. The full color group expression for $V(\sigma)$ is given in the Appendix. In arriving at that we have reproduced the two loop Yang-Mills theory result of [51] and the subsequent extension to N_f massless quarks [52]. The potential is as one would expect in that the three loop term is cubic in $\overline{\ln}(\bar{g}\bar{\sigma})$.

IV. ANALYSIS

We are now in a position to refine the two loop estimates for $\langle \frac{1}{2}A^{a2}_\mu \rangle$ given in [51,52] and from them to deduce a value for the gluon mass. The analysis in this section will focus again on $SU(3)$ with $N_f = 3$ in order to illustrate the method but we will record results for the gluon mass for other values of N_f as well as for $SU(2)$. First, to assist with this we record the numerical expression for the effective potential which is

$$V(\bar{\sigma})|^{SU(3)}_{N_f=3} = [1.333333 + [6.000000\overline{\ln}(\bar{g}\bar{\sigma}) - 19.679012]a + [-13.500000\overline{\ln}^2(\bar{g}\bar{\sigma}) + 122.888889\overline{\ln}(\bar{g}\bar{\sigma}) - 78.871262]a^2 + [60.750000\overline{\ln}^3(\bar{g}\bar{\sigma}) - 883.500000\overline{\ln}^2(\bar{g}\bar{\sigma}) + 1701.846389\overline{\ln}(\bar{g}\bar{\sigma}) - 3902.054942]a^3]\bar{\sigma}^2 + O(a^4). \tag{4.1}$$

The stationary points are deduced by solving

$$\frac{dV}{d\bar{\sigma}} = 0 \tag{4.2}$$

and from (4.1) we have

$$\left.\frac{dV}{d\bar{\sigma}}\right|^{SU(3)}_{N_f=3} = [2.666667 + [12.000000\overline{\ln}(\bar{g}\bar{\sigma}) - 33.358025]a + [-27.000000\overline{\ln}^2(\bar{g}\bar{\sigma}) + 218.777778\overline{\ln}(\bar{g}\bar{\sigma}) - 34.853636]a^2 + [121.500000\overline{\ln}^3(\bar{g}\bar{\sigma}) - 1584.750000\overline{\ln}^2(\bar{g}\bar{\sigma}) + 1636.692777\overline{\ln}(\bar{g}\bar{\sigma}) - 6102.263495]a^3]\bar{\sigma} + O(a^4). \tag{4.3}$$

In order to extract the location of the stationary point we follow the prescription given in [46,47,51] and set the scale to be where the logarithm vanishes which is

$$\bar{g}\bar{\sigma} = \mu^2 \tag{4.4}$$

which produces several solutions. There is one stationary point at $\bar{\sigma} = 0$ which corresponds to the usual perturbative vacuum with $V(0) = 0$. At one and higher loops this is a local maximum but in the absence of loop corrections it a minimum. Nonzero solutions for $\bar{\sigma}$ result from the remaining cubic in a and these correspond to the global minimum of the potential. We have solved for the coupling constant values numerically and the $SU(3)$ results are given in Table I with $a^{(L)}$ indicating the solution at L loops. In [51,52] a different convention was used for the coupling constant which was denoted by y. It is related to a by factor of N_c. Here we prefer to use a as the variable since the rescaling by N_c or in effect C_A is arbitrary and ineffectual. Moreover additional rank 4 Casimirs appear in the effective potential at three loops as is evident in (A7).

In Table I there is no solution for the coupling at the two loop stationary point for $N_f = 5$ and the $SU(3)$ group since the quadratic equation in a produces complex conjugate roots. For the case of $SU(2)$ the situation is similar but arises at a lower value of N_f with those stationary point couplings given in Table II. While both tables indicate that the nonzero stationary point coupling decreases with loop order, what is more important is the behavior of the effective gluon mass induced by the nonzero value of $\langle\bar{\sigma}\rangle$. Therefore we have to translate the stationary point couplings to a value for the gluon mass. This will be a two stage process. First using the values found for a at the stationary point of the three loop potential we obtain

TABLE I. Values of $SU(3)$ coupling constants at the minimum of the potential for N_f massless quarks.

N_f	$a^{(1)}$	$a^{(2)}$	$a^{(3)}$
0	0.064171	0.046493	0.035626
2	0.073973	0.061090	0.044562
3	0.079941	0.074190	0.051766
4	0.086787	0.100128	0.063391
5	0.094641	———	0.090027

TABLE II. Values of $SU(2)$ coupling constants at the minimum of the potential for N_f massless quarks.

N_f	$a^{(1)}$	$a^{(2)}$	$a^{(3)}$
0	0.096257	0.069739	0.053594
2	0.120805	0.111985	0.078461
3	0.137908	0.217124	0.113177
4	0.138742	———	———
5	0.146341	———	———

estimates for $\bar{g}\langle\bar{\sigma}\rangle$ using the relation (4.4) before repeating the process provided in [51,52]. This is based on the relation between the running coupling constant and a mass scale in units of the Λ parameter. As we have focused on the $\overline{\text{MS}}$ scheme throughout, our reference scale will therefore be $\Lambda_{\overline{\text{MS}}}$. Solving the first order differential equation that defines the β-function in a perturbative way allows us to either express the coupling constant as a function of mass which we denote by $a^{(L)}(m)$ at each loop order L or $\bar{g}\langle\bar{\sigma}\rangle$ as a function of the coupling constant. We will use $m^{(L)}(a)$ to denote a generic mass scale. For reference to three loops the explicit expressions are

$$\begin{aligned}
a^{(1)}(m) &= -\frac{1}{\beta_0 \ln(\frac{m^2}{\Lambda^2})}, \\
a^{(2)}(m) &= -\frac{1}{\beta_0 \ln(\frac{m^2}{\Lambda^2})} - \frac{\beta_1 \ln(\ln(\frac{m^2}{\Lambda^2}))}{\beta_0^3 \ln^2(\frac{m^2}{\Lambda^2})}, \\
a^{(3)}(m) &= -\frac{1}{\beta_0 \ln(\frac{m^2}{\Lambda^2})} - \frac{\beta_1 \ln(\ln(\frac{m^2}{\Lambda^2}))}{\beta_0^3 \ln^2(\frac{m^2}{\Lambda^2})} \\
&\quad - \left[\beta_1^2 \left[\ln^2\left(\ln\left(\frac{m^2}{\Lambda^2}\right)\right) - \ln\left(\ln\left(\frac{m^2}{\Lambda^2}\right)\right) - 1\right]\right. \\
&\quad \left. + \beta_0\beta_2\right] \frac{1}{\beta_0^5 \ln^3(\frac{m^2}{\Lambda^2})}
\end{aligned} \tag{4.5}$$

and

$$\begin{aligned}
m^{(1)}(a) &= \Lambda \exp\left[-\frac{1}{2\beta_0 a}\right], \\
m^{(2)}(a) &= \Lambda \exp\left[-\frac{1}{2\beta_0 a} - \frac{\beta_1}{2\beta_0^2}\ln(-\beta_0 a)\right], \\
m^{(3)}(a) &= \Lambda \exp\left[-\frac{1}{2\beta_0 a} - \frac{\beta_1}{2\beta_0^2}\ln(-\beta_0 a) + \frac{1}{2\beta_0^3}[\beta_1^2 - \beta_0\beta_2]a\right]
\end{aligned} \tag{4.6}$$

for any renormalization scheme. Specifically the β-function coefficients are [85–90]

$$\begin{aligned}
\beta_0 &= -\left[\frac{11}{3}C_A - \frac{4}{3}T_F N_f\right], \\
\beta_1 &= -\left[\frac{34}{3}C_A^2 - 4T_F C_F N_f - \frac{20}{3}T_F N_f C_A\right], \\
\beta_2 &= -\left[\frac{2857}{54}C_A^3 + 2C_F^2 T_F N_f - \frac{205}{9}C_F C_A T_F N_f\right. \\
&\quad \left. - \frac{1415}{27}C_A^2 T_F N_f + \frac{44}{9}C_F T_F^2 N_f^2 + \frac{158}{27}C_A T_F^2 N_f^2\right]
\end{aligned} \tag{4.7}$$

for reference. Using the values for $a^{(L)}$ given in Tables I and II it is a straightforward exercise to substitute them into

the right side of (4.6). To deduce estimates for $\bar{g}\langle\bar{\sigma}\rangle$ from (4.5) requires more work in that we searched for a value of $\frac{m}{\Lambda}$ that gave the respective values of $a^{(L)}$ in each of these tables. One reason for using two methods rests in the fact that we are working with a truncation by loop order. If the all orders expressions for (4.5) and (4.6) were both available then each would be the precise inverse function of the other. So the solution to either would give the same value for the mass. In the truncated case the discrepancy between them would be a rough measure of the accuracy at each loop order. The results of this analysis for both approaches are recorded in Tables III and IV for $SU(3)$ and the respective $SU(2)$ estimates are provided in Tables V and VI. Several initial comments on Tables III to VI are apt. First the estimates up to $N_f = 3$ at one and two loops in Tables IV and VI are in agreement with [51,52] while the remainder are new. We have chosen to include higher values of N_f to illustrate that at a certain point, which differs for each group, there is not always a solution for the coupling at a stationary point. Next the estimates for $\bar{g}\langle\bar{\sigma}\rangle$ at one loop in the pair of tables for each group are identical. This follows trivially from the fact that $a^{(1)}(m)$ and $m^{(1)}(a)$ are formal inverses of each other which is evident from (4.5) and (4.6).

TABLE III. Values of $\bar{g}\langle\bar{\sigma}\rangle/\Lambda_{\overline{\rm MS}}$ for $SU(3)$ at L loops using (4.5).

N_f	$L=1$	$L=2$	$L=3$
0	2.030604	2.003773	2.591158
2	2.012200	1.878750	2.418769
3	2.003627	1.802659	2.297279
4	1.996403	1.702877	2.120771
5	1.991927	———	1.806990

TABLE IV. Values of $\bar{g}\langle\bar{\sigma}\rangle/\Lambda_{\overline{\rm MS}}$ for $SU(3)$ at L loops using (4.6).

N_f	$L=1$	$L=2$	$L=3$
0	2.030604	2.124240	2.654008
2	2.012200	1.986479	2.467973
3	2.003627	1.890028	2.334335
4	1.996403	1.744687	2.142946
5	1.991927	———	1.826447

TABLE V. Values of $\bar{g}\langle\bar{\sigma}\rangle/\Lambda_{\overline{\rm MS}}$ for $SU(2)$ at L loops using (4.5).

N_f	$L=1$	$L=2$	$L=3$
0	2.030604	2.003773	2.585258
2	1.993346	1.793178	2.269245
3	1.973484	1.624988	1.950830
4	2.164616	———	———
5	2.349416	———	———

TABLE VI. Values of $\bar{g}\langle\bar{\sigma}\rangle/\Lambda_{\overline{\rm MS}}$ for $SU(2)$ at L loops using (4.6).

N_f	$L=1$	$L=2$	$L=3$
0	2.030604	2.124240	2.647960
2	1.993346	1.882611	2.306476
3	1.973484	1.584461	1.969801
4	2.164616	———	———
5	2.349416	———	———

The second stage in the process to estimate the gluon mass is to translate the values of $\bar{g}\langle\bar{\sigma}\rangle$ into the effective mass which is defined by

$$m^2_{\rm eff} = \frac{\langle\bar{\sigma}\rangle}{g\zeta(a)} \tag{4.8}$$

based on (3.6). This definition differs from that used in [46,47,51,52] which took the value of $\bar{g}\langle\bar{\sigma}\rangle$ for the gluon mass. If one were to use that approach here it is evident that there would be convergence concerns given the jump in the three loop values in comparison with the two loop ones from examining Tables III to VI for both groups. In light of this we have taken (4.8) as a more appropriate quantity to use. Consequently we have to compute a value for $\zeta(a)$ for each group and N_f value which is achieved by evaluating $\zeta(a)$ using the coupling constants given in Tables I and II. However naively substituting those numbers into the perturbative expression for $1/(a\zeta(a))$, either (3.3) or (A3), will lead to convergence issues. Therefore to deduce each adjustment factor we have calculated Padé approximants to $1/(a\zeta(a))$ using the one, two, and three loop terms of (3.3) and (A3) to find the numbers to multiply each entry in Tables III to VI. In particular we have used the [0, 1], [0, 2], and [1, 2] Padé approximants at the respective orders. For the $SU(3)$ case we can also include the values of $\Lambda_{\overline{\rm MS}}$ which are summarized in Table VII. Therefore combining the three values of $\bar{g}\bar{\sigma}$ and $1/(a\zeta(a))$ we arrive at the values given in Tables VIII and IX. The errors are derived from those given in Table VII.

TABLE VII. Values of $\Lambda_{\overline{\rm MS}}$ in MeV.

N_f	$\Lambda_{\overline{\rm MS}}$	Reference
0	224^{+8}_{-5}	[91]
2	294^{+10}_{-10}	[92]
3	339^{+10}_{-10}	[93]
4	296^{+10}_{-10}	[93]
5	213^{+8}_{-8}	[93]

TABLE VIII. Values of $m_{\rm eff}$ in MeV for $SU(3)$ at L loops based on Table III.

N_f	$L=1$	$L=2$	$L=3$
0	333^{+12}_{-6}	303^{+11}_{-7}	319^{+12}_{-7}
2	432^{+15}_{-14}	354^{+12}_{-12}	355^{+12}_{-12}
3	495^{+15}_{-15}	374^{+11}_{-11}	369^{+10}_{-11}
4	430^{+14}_{-15}	280^{+9}_{-9}	287^{+10}_{-9}
5	308^{+11}_{-12}	———	166^{+6}_{-7}

TABLE IX. Values of $m_{\rm eff}$ in MeV for $SU(3)$ at L loops based on Table IV.

N_f	$L=1$	$L=2$	$L=3$
0	333^{+12}_{-6}	321^{+12}_{-7}	327^{+12}_{-7}
2	432^{+15}_{-14}	374^{+13}_{-13}	361^{+13}_{-11}
3	495^{+15}_{-15}	392^{+14}_{-11}	375^{+11}_{-12}
4	430^{+14}_{-15}	287^{+12}_{-10}	290^{+10}_{-9}
5	308^{+11}_{-12}	———	168^{+6}_{-7}

What is evident from both Tables VIII and IX is that there is a degree of stability in the two and three loop effective gluon mass estimates up to $N_f = 4$. This is probably not unrelated to the coupling constants at these orders being smaller than the one loop value for $N_f \neq 0$ and therefore more within the range of perturbative reliability. Another feature is that the mass increases up to $N_f = 3$. This behavior though needs to be tempered by recalling that we have assumed the quarks are massless. The inclusion of a quark mass would undoubtedly complicate the structure of the effective potential and thereby affect the effective gluon mass estimates. As we chose to gauge the truncation discrepancy by extracting a value for $\bar{g}\langle\bar{\sigma}\rangle$ from the couplings in two different ways it is worth commenting on this. If one compares say the $N_f = 0$ two loop effective mass values in Tables VIII and IX there is roughly a 6% difference. This reduces to around 2.5% at three loops. A similar narrowing is present for the other N_f cases. One main feature is that in the Yang-Mills theory case there is a marked degree of consistency at each loop order. One way of providing a rough ballpark estimate of the effective gluon mass using the LCO approach is to average the three loop value in the tables. For example for Yang-Mills theory this would give $m_{\rm eff} = 323$ MeV.

Other methods have produced gluon mass estimates which we mention for balance. For instance, the study of [43] investigated the effect of including the Gribov mass [10], in a model which also included a gluon mass operator. The main observation was that both mass scales were roughly equal and around 500 MeV. In particular the two mass parameters appear in the gluon propagator that can be derived from various modifications of Gribov's original action [10]. Zwanziger's reformulation of the Gribov action as a local renormalizable one [11–21] provided the basis for various extensions that included a gluon mass parameter such as [22–24]. While such a study produces mass that is of the accepted magnitude this was achieved by fitting to a classical propagator and therefore omitted quantum effects. This has been extended in later investigations. For instance, one and two loop corrections to the gluon propagator have been calculated using the Landau gauge Lagrangian with a gluon mass term which is justified by the interpretation of the mass being related to Gribov copies [35–42]. The subsequent gluon mass estimates were deduced by fitting the one and two loop propagators, that were calculated analytically [37,40–42], against Landau gauge lattice data producing respective estimates of 350 and 330 MeV. A more recent study [44] using a functional renormalization group approach computed the effective potential of the field strength. From the value of the resulting field strength condensate an effective gluon mass gap of 0.312(27) GeV was found which was commensurate with the lattice value of 0.3536(11) GeV for the mass gap derived from the lattice data of [94]. These two values, as well as a similar gluon mass estimate [37,40–42], extracted from different lattice data, indicates a relative degree of consistency from various directions. Therefore it is interesting that the LCO method produced a three loop gluon mass estimate that is very similar to these independent Lagrangian based methods.

We complete our analysis by providing similar estimates for the $SU(2)$ effective gluon mass. The situation differs here in that we do not have values for $\Lambda_{\overline{\rm MS}}$ and so cannot give mass estimates in any physical units. Instead we have provided $m_{\rm eff}/\Lambda_{\overline{\rm MS}}$ for the three values of N_f where there were coupling constant solutions at each loop order. These are recorded in Tables X and XI where the respective values from the Padé approximants to $1/(a\zeta(a))$ have been included. A similar pattern to the $SU(3)$ case is apparent. There is a degree of stability for Yang-Mills theory across loop orders for both tables. For $N_f = 2$ the two and three loop estimates are similar but for $N_f = 3$ there is less consistency across loop order. This is parallel to the $N_f = 4$ and 5 cases for $SU(3)$ since the latter is the value before which there are no two or three loop solutions for the

TABLE X. Values of $m_{\rm eff}/\Lambda_{\overline{\rm MS}}$ for $SU(2)$ at L loops based on Table V.

N_f	$L=1$	$L=2$	$L=3$
0	1.488526	1.352525	1.446185
2	1.454108	1.098230	1.128747
3	1.434460	0.761928	0.937949

TABLE XI. Values of $m_{\rm eff}/\Lambda_{\overline{\rm MS}}$ for $SU(2)$ at L loops based on Table VI.

N_f	$L=1$	$L=2$	$L=3$
0	1.488526	1.433839	1.481260
2	1.454108	1.153003	1.147266
3	1.434460	0.742926	0.946343

minimum of the effective potential. The three loop effective gluon mass estimate in that situation appears to be out of line with the pattern of values for lower N_f. This is perhaps an indicator of the loss of a minimal effective potential solution for higher N_f and this appears to be borne out for the $SU(2)$ group as well.

V. DISCUSSION

We have applied the LCO formalism to a new loop order for any theory and in particular a gauge theory. Our main focus has centered on QCD with N_f massless quarks. The key observation is that for Yang-Mills theory the three loop corrections to the effective gluon mass derived from the minimum of the effective potential demonstrate a degree of convergence. For the $SU(3)$ color group this is centered roughly around the value of 323 MeV for the effective mass. This is not inconsistent, for instance, with values from other methods such as extracting a mass by fitting perturbative gluon propagators to lattice data or functional renormalization group techniques. The same analysis showed that this apparent convergence was evident for $SU(2)$ Yang-Mills theory as well. The situation for nonzero N_f was not as clear cut. This was primarily because, as noted in [52], there was a marked difference between the one and two loop values of the effective mass computed there albeit with a different definition from the one used here. With the current definition (4.8) this is also apparent but interestingly Tables VIII and IX support the notion that the two and three loop values for the effective mass have stabilized when further corrections are included. Of course this is in the simplified scenario of massless quarks which is not truly realistic. What would be needed is a generalization of the LCO method to induce quark masses from an extended effective potential. This does not seem straightforward if one naively examines the core formalism. The LCO construction for the gluon mass operator benefits from this having mass dimension 2 with an associated mass dimension 2 source field that therefore requires a quadratic source term on renormalizability grounds. Using the same dimensional analysis the quark mass operator would have dimension 3 meaning its source field would be dimension 1. Therefore aside from the mixing of the two types of sources to produce a cubic term, quartic quark mass operator source terms would be necessary on renormalizability grounds. The technical issues of accommodating this within the LCO formalism may not be insurmountable but would require new insights to find the effective potential.

In terms of future directions given that the core renormalization group functions of QCD are known at five loops in the $\overline{\rm MS}$ scheme [55–58], the techniques are already available in principle to deduce the next term in the series for $\zeta(a)$. This would require a five loop computation of the J correlation function. In addition the approach of [57] to renormalize QCD using a vacuum bubble expansion means that all the core four loop Feynman integrals that are necessary to compute the four loop graphs of the effective potential are known. Therefore extending our analysis to the next loop order would seem viable in the foreseeable future. From another point of view it would be interesting to apply the LCO Lagrangian to other problems such as the evaluation of 2- and 3-point functions akin to that studied in [37,40–42]. The reasoning would be to see if the mass estimate extracted here was consistent with lattice data as well as testing the effect the extra interactions present in (2.18) have. Finally we recall that one of the early observations that led to the interest in studying the value of $\langle \frac{1}{2} A_\mu^{a2} \rangle$ in the Landau gauge arose in lattice and other studies [95–99]. It was noted that $O(1/p^2)$ power corrections arose in operator product expansion measurements. This ran counter to expectations that the leading correction would be $O(1/(p^2)^2)$. With the general acceptance that an effective gluon mass lurks in Yang-Mills theory the LCO Lagrangian might be the tool to formally reexamine the operator product expansion.

The data representing the main results here are accessible from [75].

ACKNOWLEDGMENTS

This work was carried out with the support of STFC through the Consolidated Grant ST/T000988/1. The diagrams were prepared with the AXODRAW package [100].

APPENDIX: EXPRESSIONS FOR ARBITRARY COLOR GROUP

As the main analysis in the body of the article centered on the $SU(3)$ color group and $N_f = 3$ we devote this section to recording the corresponding expressions for an arbitrary group. First the counterterm associated with the source field is given to three loops by

$$\begin{aligned}
\delta\zeta = & \left[-\frac{3}{2\epsilon} + \left[[35C_A - 16N_fT_F]\frac{1}{8\epsilon^2} + [32N_fT_F - 139C_A]\frac{1}{12\epsilon} \right] a \right. \\
& + \left[[584C_AN_fT_F - 665C_A^2 - 128N_f^2T_F^2]\frac{1}{48\epsilon^3} \right. \\
& + [6629C_A^2 - 4280C_AN_fT_F - 576C_FN_fT_F + 512N_f^2T_F^2]\frac{1}{144\epsilon^2} \\
& + [27648\zeta_3C_AN_fT_F + 17524C_AN_fT_F - 6237\zeta_3C_A^2 - 71551C_A^2 - 27648\zeta_3C_FN_fT_F \\
& \left. + 33120C_FN_fT_F + 1280N_f^2T_F^2]\frac{1}{864\epsilon} \right] a^2 \\
& + \left[[52535C_A^3 - 67416C_A^2N_fT_F + 28800C_AN_f^2T_F^2 - 4096N_f^3T_F^3]\frac{1}{1152\epsilon^4} \right. \\
& + [1342920C_A^2N_fT_F - 1274497C_A^3 + 181728C_AC_FN_fT_F - 418176C_AN_f^2T_F^2 \\
& - 78336C_FN_f^2T_F^2 + 32768N_f^3T_F^3]\frac{1}{6912\epsilon^3} \\
& + [488349\zeta_3C_A^3 + 8136934C_A^3 - 2243808\zeta_3C_A^2N_fT_F - 5991276C_A^2N_fT_F \\
& + 1997568\zeta_3C_AC_FN_fT_F - 3516336C_AC_FN_fT_F + 884736\zeta_3C_AN_f^2T_F^2 \\
& + 824256C_AN_f^2T_F^2 + 31104C_F^2N_fT_F - 884736\zeta_3C_FN_f^2T_F^2 + 1301760C_FN_f^2T_F^2 + 40960N_f^3T_F^3]\frac{1}{20736\epsilon^2} \\
& + [988362\zeta_4C_A^3 - 7330584\zeta_3C_A^3 + 5416200\zeta_5C_A^3 - 19251711C_A^3 + 21050496\zeta_3C_A^2N_fT_F \\
& - 4860864\zeta_4C_A^2N_fT_F - 4976640\zeta_5C_A^2N_fT_F + 7469896C_A^2N_fT_F - 8861184\zeta_3C_AC_FN_fT_F \\
& + 4492800\zeta_4C_AC_FN_fT_F - 11612160\zeta_5C_AC_FN_fT_F + 18097952C_AC_FN_fT_F - 3723264\zeta_3C_AN_f^2T_F^2 \\
& + 1769472\zeta_4C_AN_f^2T_F^2 - 278656C_AN_f^2T_F^2 - 8460288\zeta_3C_F^2N_fT_F + 14376960\zeta_5C_F^2N_fT_F \\
& - 4405248C_F^2N_fT_F + 3317760\zeta_3C_FN_f^2T_F^2 - 1769472\zeta_4C_FN_f^2T_F^2 - 1636864C_FN_f^2T_F^2 \\
& \left. \left. - 196608\zeta_3N_f^3T_F^3 + 65536N_f^3T_F^3]\frac{1}{27648\epsilon} \right] a^3 \right] N_A + O(a^4) \qquad \text{(A1)}
\end{aligned}$$

which is translated to its renormalization group function

$$\begin{aligned}
\delta(a) = & \left[-3 + [32N_fT_F - 139C_A]\frac{a}{3} \right. \\
& + [27648\zeta_3C_AN_fT_F - 6237\zeta_3C_A^2 - 71551C_A^2 + 17524C_AN_fT_F - 27648\zeta_3C_FN_fT_F \\
& + 33120C_FN_fT_F + 1280N_f^2T_F^2]\frac{a^2}{144} \\
& + [5416200\zeta_5C_A^3 + 988362\zeta_4C_A^3 - 7330584\zeta_3C_A^3 - 19251711C_A^3 \\
& + 21050496\zeta_3C_A^2N_fT_F - 4860864\zeta_4C_A^2N_fT_F - 4976640\zeta_5C_A^2N_fT_F \\
& + 7469896C_A^2N_fT_F - 8861184\zeta_3C_AC_FN_fT_F + 4492800\zeta_4C_AC_FN_fT_F \\
& - 11612160\zeta_5C_AC_FN_fT_F + 18097952C_AC_FN_fT_F - 3723264\zeta_3C_AN_f^2T_F^2 \\
& + 1769472\zeta_4C_AN_f^2T_F^2 - 278656C_AN_f^2T_F^2 - 8460288\zeta_3C_F^2N_fT_F \\
& + 14376960\zeta_5C_F^2N_fT_F - 4405248C_F^2N_fT_F + 3317760\zeta_3C_FN_f^2T_F^2 \\
& \left. - 1769472\zeta_4C_FN_f^2T_F^2 - 1636864C_FN_f^2T_F^2 - 196608\zeta_3N_f^3T_F^3 + 65536N_f^3T_F^3]\frac{a^3}{3456} \right] N_A + O(a^4). \qquad \text{(A2)}
\end{aligned}$$

One reason for noting the counterterm was to give assurance that the derivation of $\delta(a)$ was consistent with the renormalization group formalism. By this we mean that the double and triple poles in ϵ are not independent but determined by the simple poles at lower loop orders. Equipped with this the expression for $\zeta(a)$ can be deduced from (2.10) leading to

$$
\begin{aligned}
\frac{1}{\zeta(a)} = {} & \left[\left[\frac{13}{9}C_A - \frac{8}{9}T_F N_f\right]a\right. \\
& + \left[\frac{105}{4}C_F C_A^2\lambda_2 - \frac{8129}{1296}C_A^2 - \frac{105}{16}C_A^3\lambda_2 - \frac{3}{4}C_F C_A + \frac{557}{81}T_F C_A N_f - \frac{4}{3}T_F C_F N_f - \frac{128}{81}T_F^2 N_f^2\right]a^2 \\
& + \left[\frac{1459}{36}C_A^4\lambda_3 - \frac{15005}{1728}C_A^3 - \frac{4795}{128}C_A^4\lambda_2 - \frac{11025}{128}C_A^5\lambda_2^2 - \frac{629}{144}C_F C_A^2 + \frac{950}{9}C_F C_A^3\lambda_3 - \frac{245}{4}C_F C_A^3\lambda_2\right. \\
& + \frac{11025}{16}C_F C_A^4\lambda_2^2 + \frac{8}{3}C_F^2 C_A - \frac{1463}{3}C_F^2 C_A^2\lambda_3 + \frac{6755}{8}C_F^2 C_A^2\lambda_2 - \frac{11025}{8}C_F^2 C_A^3\lambda_2^2 - \frac{20275}{1944}T_F C_A^2 N_f \\
& + \frac{2311}{81}T_F C_F C_A N_f + \frac{10}{9}T_F C_F^2 N_f + \frac{3674}{243}T_F^2 C_A N_f^2 - \frac{1880}{81}T_F^2 C_F N_f^2 - \frac{896}{243}T_F^3 N_f^3 - \frac{1661}{144}\zeta_3 C_A^3 \\
& + \frac{763}{6}\zeta_3 C_A^4\lambda_3 + \frac{20}{3}\zeta_3 C_F C_A^2 - \frac{380}{3}\zeta_3 C_F C_A^3\lambda_3 + \frac{1343}{54}\zeta_3 T_F C_A^2 N_f - \frac{592}{27}\zeta_3 T_F C_F C_A N_f \\
& \left. - \frac{512}{27}\zeta_3 T_F^2 C_A N_f^2 + \frac{512}{27}\zeta_3 T_F^2 C_F N_f^2\right]a^3 \\
& + \left[\frac{256}{27}N_f\frac{d_F^{abcd}d_A^{abcd}}{N_A} - \frac{659}{864}\frac{d_A^{abcd}d_A^{abcd}}{N_A} - \frac{352}{27}N_f^2\frac{d_F^{abcd}d_F^{abcd}}{N_A} + \frac{659}{32}C_A\lambda_4\frac{d_A^{abcd}d_A^{abcd}}{N_A} - 256C_A N_f\lambda_4\frac{d_F^{abcd}d_A^{abcd}}{N_A}\right. \\
& + 352C_A N_f^2\lambda_4\frac{d_F^{abcd}d_F^{abcd}}{N_A} - \frac{5778875537}{53747712}C_A^4 - \frac{19964625}{8192}C_A^5\lambda_4 + \frac{24803}{36}C_A^5\lambda_3 + \frac{176715}{1024}C_A^5\lambda_2 - \frac{305025}{256}C_A^6\lambda_2^2 \\
& - \frac{1157625}{1024}C_A^7\lambda_2^3 + \frac{14933}{1024}C_F C_A^3 - \frac{20457603}{1024}C_F C_A^4\lambda_4 + \frac{67735}{12}C_F C_A^4\lambda_3 - \frac{1689905}{768}C_F C_A^4\lambda_2 + \frac{591675}{128}C_F C_A^5\lambda_2^2 \\
& + \frac{3472875}{256}C_F C_A^6\lambda_2^3 + \frac{48155}{2304}C_F^2 C_A^2 + \frac{550551}{256}C_F^2 C_A^3\lambda_4 + \frac{15637}{9}C_F^2 C_A^3\lambda_3 - \frac{520135}{96}C_F^2 C_A^3\lambda_2 + \frac{40425}{2}C_F^2 C_A^4\lambda_2^2 \\
& - \frac{3472875}{64}C_F^2 C_A^5\lambda_2^3 - \frac{203}{96}C_F^3 C_A + \frac{3016773}{32}C_F^3 C_A^2\lambda_4 - \frac{138985}{3}C_F^3 C_A^2\lambda_3 + \frac{1100015}{24}C_F^3 C_A^2\lambda_2 - \frac{628425}{8}C_F^3 C_A^3\lambda_2^2 \\
& + \frac{1157625}{16}C_F^3 C_A^4\lambda_2^3 + \frac{215810801}{1679616}T_F C_A^3 N_f + \frac{3323423}{23328}T_F C_F C_A^2 N_f - \frac{75553}{648}T_F C_F^2 C_A N_f + 6T_F C_F^3 N_f \\
& - \frac{1759765}{17496}T_F^2 C_A^2 N_f^2 - \frac{22360}{729}T_F^2 C_F C_A N_f^2 + \frac{6940}{81}T_F^2 C_F^2 N_f^2 + \frac{310736}{6561}T_F^3 C_A N_f^3 - \frac{33488}{729}T_F^3 C_F N_f^3 \\
& - \frac{62464}{6561}T_F^4 N_f^4 + \frac{3395}{128}\zeta_5\frac{d_A^{abcd}d_A^{abcd}}{N_A} - 20\zeta_5 N_f\frac{d_F^{abcd}d_A^{abcd}}{N_A} - \frac{91665}{128}\zeta_5 C_A\lambda_4\frac{d_A^{abcd}d_A^{abcd}}{N_A} \\
& + 540\zeta_5 C_A N_f\lambda_4\frac{d_F^{abcd}d_A^{abcd}}{N_A} + \frac{4608325}{27648}\zeta_5 C_A^4 - \frac{2612565}{1024}\zeta_5 C_A^5\lambda_4 + \frac{2565}{16}\zeta_5 C_F C_A^3 - \frac{202635}{16}\zeta_5 C_F C_A^4\lambda_4 \\
& - \frac{1485}{8}\zeta_5 C_F^2 C_A^2 + \frac{117315}{8}\zeta_5 C_F^2 C_A^3\lambda_4 - \frac{47035}{216}\zeta_5 T_F C_A^3 N_f - \frac{1930}{9}\zeta_5 T_F C_F C_A^2 N_f + \frac{7580}{27}\zeta_5 T_F C_F^2 C_A N_f \\
& + \frac{320}{3}\zeta_5 T_F^2 C_A^2 N_f^2 + \frac{2240}{9}\zeta_5 T_F^2 C_F C_A N_f^2 - \frac{8320}{27}\zeta_5 T_F^2 C_F^2 N_f^2 + \frac{13247}{576}\zeta_4 C_A^4 - \frac{7625}{54}\zeta_4 T_F C_A^3 N_f \\
& + \frac{3172}{27}\zeta_4 T_F C_F C_A^2 N_f + \frac{3775}{27}\zeta_4 T_F^2 C_A^2 N_f^2 - \frac{3616}{27}\zeta_4 T_F^2 C_F C_A N_f^2 - \frac{1024}{27}\zeta_4 T_F^3 C_A N_f^3 + \frac{1024}{27}\zeta_4 T_F^3 C_F N_f^3 \\
& + \frac{989}{72}\zeta_3\frac{d_A^{abcd}d_A^{abcd}}{N_A} - \frac{688}{9}\zeta_3 N_f\frac{d_F^{abcd}d_A^{abcd}}{N_A} + \frac{256}{9}\zeta_3 N_f^2\frac{d_F^{abcd}d_F^{abcd}}{N_A} - \frac{2967}{8}\zeta_3 C_A\lambda_4\frac{d_A^{abcd}d_A^{abcd}}{N_A} \\
& \left. + 2064\zeta_3 C_A N_f\lambda_4\frac{d_F^{abcd}d_A^{abcd}}{N_A} - 768\zeta_3 C_A N_f^2\lambda_4\frac{d_F^{abcd}d_F^{abcd}}{N_A} - \frac{21102833}{248832}\zeta_3 C_A^4 - \frac{14781555}{1024}\zeta_3 C_A^5\lambda_4\right.
\end{aligned}
$$

$$+\frac{12971}{6}\zeta_3 C_A^5\lambda_3+\frac{36435}{32}\zeta_3 C_A^5\lambda_2-\frac{16405}{128}\zeta_3 C_F C_A^3-\frac{2339901}{128}\zeta_3 C_F C_A^4\lambda_4+\frac{19855}{2}\zeta_3 C_F C_A^4\lambda_3$$
$$-\frac{91245}{16}\zeta_3 C_F C_A^4\lambda_2+\frac{4795}{48}\zeta_3 C_F^2 C_A^2+\frac{508365}{16}\zeta_3 C_F^2 C_A^3\lambda_4-\frac{36100}{3}\zeta_3 C_F^2 C_A^3\lambda_3+\frac{18375}{4}\zeta_3 C_F^2 C_A^3\lambda_2$$
$$+\frac{890945}{2592}\zeta_3 T_F C_A^3 N_f-\frac{13775}{972}\zeta_3 T_F C_F C_A^2 N_f-\frac{4378}{27}\zeta_3 T_F C_F^2 C_A N_f-\frac{45020}{243}\zeta_3 T_F^2 C_A^2 N_f^2$$
$$-\frac{16276}{243}\zeta_3 T_F^2 C_F C_A N_f^2+\frac{4928}{27}\zeta_3 T_F^2 C_F^2 N_f^2+\frac{640}{81}\zeta_3 T_F^3 C_A N_f^3-\frac{896}{243}\zeta_3 T_F^3 C_F N_f^3$$
$$+\frac{1024}{243}\zeta_3 T_F^4 N_f^4\Bigg]a^4\Bigg]\frac{1}{N_A}+O(a^5). \tag{A3}$$

This is clearly a more involved expression compared to that of the previous order given in [51,52]. The reason for this is mainly due to the four loop terms of the β-function and the gluon mass anomalous dimensions [58,101] which both involve rank 4 color Casimirs which are not present at lower loop order. These are based on the totally symmetric tensor [74]

$$d_R^{abcd}=\frac{1}{6}\mathrm{Tr}(T_R^a T_R^{(b}T_R^c T_R^{d)}) \tag{A4}$$

for an arbitrary group representation. The designation of R to be F or A indicates evaluation in either the fundamental or adjoint representations. Next we have

$$Z_\zeta^{-1}=1+\left[\frac{13}{6}C_A-\frac{4}{3}T_F N_f\right]\frac{a}{\epsilon}$$
$$+\left[\left[T_F C_A N_f-\frac{13}{8}C_A^2\right]\frac{1}{\epsilon^2}+\left[\frac{703}{96}C_A^2-\frac{315}{32}C_A^3\lambda_2-\frac{9}{8}C_F C_A+\frac{315}{8}C_F C_A^2\lambda_2-\frac{23}{6}T_F C_A N_f-2T_F C_F N_f\right]\frac{1}{\epsilon}\right]a^2$$
$$+\left[\left[\frac{403}{144}C_A^3-\frac{22}{9}T_F C_A^2 N_f+\frac{4}{9}T_F^2 C_A N_f^2\right]\frac{1}{\epsilon^3}\right.$$
$$+\left[\frac{945}{64}C_A^4\lambda_2-\frac{521}{64}C_A^3+\frac{27}{16}C_F C_A^2-\frac{945}{16}C_F C_A^3\lambda_2+\frac{61}{12}T_F C_A^2 N_f\right.$$
$$\left.+\frac{40}{9}T_F C_F C_A N_f-\frac{2}{3}T_F^2 C_A N_f^2-\frac{8}{9}T_F^2 C_F N_f^2\right]\frac{1}{\epsilon^2}$$
$$+\left[\frac{113515}{3456}C_A^3+\frac{1459}{24}C_A^4\lambda_3-\frac{24045}{256}C_A^4\lambda_2-\frac{33075}{256}C_A^5\lambda_2^2-\frac{1043}{96}C_F C_A^2+\frac{475}{3}C_F C_A^3\lambda_3\right.$$
$$+\frac{945}{16}C_F C_A^3\lambda_2+\frac{33075}{32}C_F C_A^4\lambda_2^2+4C_F^2 C_A-\frac{1463}{2}C_F^2 C_A^2\lambda_3+\frac{20265}{16}C_F^2 C_A^2\lambda_2-\frac{33075}{16}C_F^2 C_A^3\lambda_2^2$$
$$-\frac{3193}{144}T_F C_A^2 N_f-\frac{1405}{54}T_F C_F C_A N_f+\frac{5}{3}T_F C_F^2 N_f+\frac{52}{27}T_F^2 C_A N_f^2+\frac{76}{27}T_F^2 C_F N_f^2-\frac{55}{8}\zeta_3 C_A^3+\frac{763}{4}\zeta_3 C_A^4\lambda_3$$
$$\left.+10\zeta_3 C_F C_A^2-190\zeta_3 C_F C_A^3\lambda_3-\frac{46}{3}\zeta_3 T_F C_A^2 N_f+\frac{40}{3}\zeta_3 T_F C_F C_A N_f\right]\frac{1}{\epsilon}\Bigg]a^3+O(a^4) \tag{A5}$$

which was defined in (2.19). Another quantity required prior to determining the effective potential is the renormalization constant

$$Z_m=1+\left[\frac{4}{3}T_F N_f-\frac{35}{12}C_A\right]\frac{a}{\epsilon}$$
$$+\left[\left[\frac{2765}{288}C_A^2+\frac{16}{9}T_F^2 N_f^2-\frac{149}{18}T_F N_f C_A\right]\frac{1}{\epsilon^2}+\left[2T_F N_f C_F-\frac{449}{96}C_A^2+\frac{35}{12}T_F N_f C_A\right]\frac{1}{\epsilon}\right]a^2+O(a^3). \tag{A6}$$

While this is already available to high loop order via the Slavnov-Taylor identity [59,61], it is provided in the conventions used to derive $V(\sigma)$ and is the source for deducing $\gamma_m(a)$.

Finally the full effective potential at three loops for the Landau gauge gluon mass operator for an arbitrary color group is

$$
\begin{aligned}
V(\sigma) = {} & \left[\frac{9}{2}\lambda_1 + \left[\frac{105}{2}C_F\lambda_2 - \frac{39}{2}C_F\lambda_1 - \frac{13}{8} - \frac{105}{8}C_A\lambda_2 - \frac{9}{4}C_A\lambda_1 + \frac{3}{4}\overline{\ln}(\bar{g}\bar{\sigma})\right]a \right. \\
& + \left[\frac{1459}{32}C_A^2\lambda_3 - \frac{7665}{64}C_A^2\lambda_2 - \frac{2373}{64}C_A^2\lambda_1 - \frac{593}{64}C_A - \frac{11025}{64}C_A^3\lambda_2^2 - \frac{247}{16}C_F\right. \\
& + \frac{475}{4}C_FC_A\lambda_3 + 210C_FC_A\lambda_2 + \frac{429}{16}C_FC_A\lambda_1 + \frac{11025}{8}C_FC_A^2\lambda_2^2 - \frac{4389}{8}C_F^2\lambda_3 \\
& + \frac{4305}{4}C_F^2\lambda_2 + \frac{39}{8}C_F^2\lambda_1 - \frac{11025}{4}C_F^2C_A\lambda_2^2 - 12\zeta_3C_A + \frac{2289}{16}\zeta_3C_A^2\lambda_3 \\
& + \frac{1377}{32}\zeta_3C_A^2\lambda_1 + 12\zeta_3C_F - \frac{285}{2}\zeta_3C_FC_A\lambda_3 - \frac{117}{2}\zeta_3C_FC_A\lambda_1 - \frac{1}{16}\zeta_2C_A \\
& + 2\zeta_2T_FN_f + \frac{99}{16}\sqrt{3}\mathrm{Ls}_2\left(\frac{2\pi}{3}\right)C_A \\
& + \left[\frac{75}{16}C_A + \frac{315}{16}C_A^2\lambda_2 + \frac{9}{4}C_F - \frac{315}{4}C_FC_A\lambda_2\right]\overline{\ln}(\bar{g}\bar{\sigma}) - \frac{9}{16}C_A\overline{\ln}^2(\bar{g}\bar{\sigma})\Bigg]a^2 \\
& + \left[\left[\frac{274995}{64}\zeta_5 + \frac{8901}{4}\zeta_3 - \frac{1977}{16}\right]\lambda_1\lambda_4\frac{d_A^{abcd}d_A^{abcd}}{N_A} + [1536 - 3240 - 12384\zeta_3]N_f\lambda_1\lambda_4\frac{d_F^{abcd}d_A^{abcd}}{N_A}\right. \\
& + [4608\zeta_3 - 2112]N_f^2\lambda_1\lambda_4\frac{d_F^{abcd}d_F^{abcd}}{N_A} \\
& - \frac{4647721}{27648}C_A^2 - \frac{6654875}{3072}C_A^3\lambda_4 + \frac{77327}{96}C_A^3\lambda_3 - \frac{162085}{384}C_A^3\lambda_2 - \frac{64193}{384}C_A^3\lambda_1 - \frac{738675}{256}C_A^4\lambda_2^2 \\
& - \frac{1157625}{512}C_A^5\lambda_2^3 - \frac{6301}{48}C_FC_A - \frac{2273067}{128}C_FC_A^2\lambda_4 + \frac{617215}{96}C_FC_A^2\lambda_3 - \frac{56245}{64}C_FC_A^2\lambda_2 \\
& + \frac{74087}{192}C_FC_A^2\lambda_1 + \frac{488775}{32}C_FC_A^3\lambda_2^2 + \frac{3472875}{128}C_FC_A^4\lambda_2^3 + \frac{1791}{32}C_F^2 + \frac{183517}{96}C_F^2C_A\lambda_4 + \frac{12711}{8}C_F^2C_A\lambda_3 \\
& - \frac{168315}{32}C_F^2C_A\lambda_2 - \frac{7579}{24}C_F^2C_A\lambda_1 + \frac{260925}{16}C_F^2C_A^2\lambda_2^2 - \frac{3472875}{32}C_F^2C_A^3\lambda_2^3 + \frac{335197}{4}C_F^3\lambda_4 \\
& - \frac{416955}{8}C_F^3\lambda_3 + \frac{1490755}{24}C_F^3\lambda_2 + \frac{1963}{24}C_F^3\lambda_1 - 124950C_F^3C_A\lambda_2^2 + \frac{1157625}{8}C_F^3C_A^2\lambda_2^3 + \frac{29257}{864}T_FC_AN_f \\
& + \frac{1903}{24}T_FC_FN_f + \frac{135}{2}\zeta_5C_A^2 - \frac{290285}{128}\zeta_5C_A^3\lambda_4 - \frac{43855}{512}\zeta_5C_A^3\lambda_1 + \frac{315}{2}\zeta_5C_FC_A - \frac{22515}{2}\zeta_5C_FC_A^2\lambda_4 \\
& - 195\zeta_5C_FC_A^2\lambda_1 - 195\zeta_5C_F^2 + 13035\zeta_5C_F^2C_A\lambda_4 + 390\zeta_5C_F^2C_A\lambda_1 + \frac{20913}{512}\zeta_4C_A^2 - \frac{4131}{64}\zeta_4C_A^3\lambda_1 \\
& - \frac{27}{4}\zeta_4C_FC_A + \frac{351}{4}\zeta_4C_FC_A^2\lambda_1 - 88\zeta_4T_FC_AN_f + 108\zeta_4T_FC_FN_f - \frac{12703}{192}\zeta_3C_A^2 - \frac{1642395}{128}\zeta_3C_A^3\lambda_4 \\
& + \frac{40439}{16}\zeta_3C_A^3\lambda_3 + \frac{36435}{16}\zeta_3C_A^3\lambda_2 + \frac{67125}{256}\zeta_3C_A^3\lambda_1 - \frac{1439}{32}\zeta_3C_FC_A - \frac{259989}{16}\zeta_3C_FC_A^2\lambda_4 + \frac{177175}{16}\zeta_3C_FC_A^2\lambda_3 \\
& - \frac{91245}{8}\zeta_3C_FC_A^2\lambda_2 - \frac{2613}{32}\zeta_3C_FC_A^2\lambda_1 + \frac{231}{2}\zeta_3C_F^2 + \frac{56485}{2}\zeta_3C_F^2C_A\lambda_4 - \frac{27075}{2}\zeta_3C_F^2C_A\lambda_3 + \frac{18375}{2}\zeta_3C_F^2C_A\lambda_2 \\
& - 299\zeta_3C_F^2C_A\lambda_1 + \frac{241}{6}\zeta_3T_FC_AN_f - \frac{263}{3}\zeta_3T_FC_FN_f - \frac{9883}{2304}\zeta_2C_A^2 + \frac{7245}{64}\zeta_2C_A^3\lambda_2 + \frac{207}{16}\zeta_2C_FC_A \\
& - \frac{7245}{16}\zeta_2C_FC_A^2\lambda_2 + \frac{6701}{288}\zeta_2T_FC_AN_f - 16\zeta_2T_FC_FN_f - \frac{16}{9}\zeta_2T_F^2N_f^2 - \frac{225}{8}\mathrm{Li}_4\left(\frac{1}{2}\right)C_A^2 + 64\mathrm{Li}_4\left(\frac{1}{2}\right)T_FC_AN_f \\
& \left. - 128\mathrm{Li}_4\left(\frac{1}{2}\right)T_FC_FN_f + \frac{4239}{256}\mathrm{Ls}_2^2\left(\frac{2\pi}{3}\right)C_A^2 - 36\mathrm{Ls}_2^2\left(\frac{2\pi}{3}\right)T_FC_AN_f + \frac{225}{32}\ln^2(2)\zeta_2C_A^2 - 16\ln^2(2)\zeta_2T_FC_AN_f\right.
\end{aligned}
$$

$$
\begin{aligned}
&+ 32\ln^2(2)\zeta_2 T_F C_F N_f - \frac{75}{64}\ln^4(2) C_A^2 + \frac{8}{3}\ln^4(2) T_F C_A N_f - \frac{16}{3}\ln^4(2) T_F C_F N_f - \frac{11}{432}\sqrt{3}\pi^3 C_A^2 \\
&+ \frac{11}{18}\sqrt{3}\pi^3 T_F C_A N_f + \frac{677}{64}\sqrt{3}\mathrm{Ls}_2\left(\frac{2\pi}{3}\right) C_A^2 + 11\sqrt{3}\mathrm{Ls}_2\left(\frac{2\pi}{3}\right) T_F C_A N_f \\
&+ \frac{10395}{64}\sqrt{3}\mathrm{Ls}_2\left(\frac{2\pi}{3}\right) C_A^3\lambda_2 + \frac{297}{16}\sqrt{3}\mathrm{Ls}_2\left(\frac{2\pi}{3}\right) C_F C_A - \frac{10395}{16}\sqrt{3}\mathrm{Ls}_2\left(\frac{2\pi}{3}\right) C_F C_A^2\lambda_2 \\
&+ \left[\frac{61787}{768} C_A^2 - \frac{1459}{16} C_A^3\lambda_3 + \frac{34965}{128} C_A^3\lambda_2 + \frac{99225}{256} C_A^4\lambda_2^2 + \frac{979}{32} C_F C_A - \frac{475}{2} C_F C_A^2\lambda_3 - \frac{8715}{16} C_F C_A^2\lambda_2 \right. \\
&- \frac{99225}{32} C_F C_A^3\lambda_2^2 - \frac{3}{16} C_F^2 + \frac{4389}{4} C_F^2 C_A\lambda_3 - \frac{17535}{8} C_F^2 C_A\lambda_2 + \frac{99225}{16} C_F^2 C_A^2\lambda_2^2 - \frac{307}{16} T_F C_A N_f \\
&- \frac{70}{3} T_F C_F N_f + \frac{1335}{64}\zeta_3 C_A^2 - \frac{2289}{8}\zeta_3 C_A^3\lambda_3 - 15\zeta_3 C_F C_A + 285\zeta_3 C_F C_A^2\lambda_3 - 16\zeta_3 T_F C_A N_f + 16\zeta_3 T_F C_F N_f \\
&- \frac{341}{384}\zeta_2 C_A^2 - \frac{485}{48}\zeta_2 T_F C_A N_f + \frac{8}{3}\zeta_2 T_F^2 N_f^2 - \frac{1023}{32}\sqrt{3}\mathrm{Ls}_2\left(\frac{2\pi}{3}\right) C_A^2 + \frac{33}{4}\sqrt{3}\mathrm{Ls}_2\left(\frac{2\pi}{3}\right) T_F C_A N_f \Big] \overline{\ln}(\bar{g}\bar{\sigma}) \\
&+ \left[\frac{2835}{32} C_F C_A^2\lambda_2 + \frac{15}{4} T_F C_A N_f + \frac{3}{2} T_F C_F N_f - \frac{1791}{128} C_A^2 - \frac{2835}{128} C_A^3\lambda_2 - \frac{81}{32} C_F C_A \right] \overline{\ln}^2(\bar{g}\bar{\sigma}) \\
&+ \left. \left[\frac{31}{32} C_A^2 - \frac{1}{4} T_F C_A N_f \right] \overline{\ln}^3(\bar{g}\bar{\sigma}) \right] a^3 \Big] N_A\bar{\sigma}^2 + O(a^4). \qquad \text{(A7)}
\end{aligned}
$$

We have used the same shorthand notation as [52] for various color group combinations but appended these with a new one, λ_4, that arises at this new loop order. These are

$$
\begin{aligned}
\lambda_1 &= \frac{1}{[13C_A - 8T_F N_f]}, \qquad \lambda_2 = \frac{1}{[35C_A - 16T_F N_f]}, \\
\lambda_3 &= \frac{1}{[19C_A - 8T_F N_f]}, \qquad \lambda_4 = \frac{1}{[79C_A - 32T_F N_f]}. \qquad \text{(A8)}
\end{aligned}
$$

For completeness we note [74]

$$
\begin{aligned}
d_F^{abcd} d_F^{abcd} &= \frac{(N_c^2-1)(N_c^4 - 6N_c^2 + 18)}{96N_c^2}, \qquad d_F^{abcd} d_A^{abcd} = \frac{N_c(N_c^2-1)(N_c^2+6)}{48}, \\
d_A^{abcd} d_A^{abcd} &= \frac{N_c^2(N_c^2-1)(N_c^2+36)}{24} \qquad \text{(A9)}
\end{aligned}
$$

for $SU(N_c)$.

[1] A. Cucchieri and T. Mendes, Proc. Sci., LATTICE2007 (**2007**) 297.
[2] I. L. Bogolubsky, E. M. Ilgenfritz, M. Müller-Preussker, and A. Sternbeck, Proc. Sci., LATTICE2007 (**2007**) 290.
[3] A. Maas, Phys. Rev. D **75**, 116004 (2007).
[4] A. Sternbeck, L. von Smekal, D. B. Leinweber, and A. G. Williams, Proc. Sci., LATTICE2007 (**2007**) 340.
[5] I. L. Bogolubsky, E. M. Ilgenfritz, M. Müller-Preussker, and A. Sternbeck, Phys. Lett. B **676**, 69 (2009).
[6] A. Cucchieri and T. Mendes, Phys. Rev. Lett. **100**, 241601 (2008).
[7] A. Cucchieri and T. Mendes, Phys. Rev. D **78**, 094503 (2008).
[8] O. Oliveira and P. J. Silva, Phys. Rev. D **79**, 031501(R) (2009).
[9] Ph. Boucaud, J. P. Leroy, A. L. Yaounac, J. Micheli, O. Pène, and J. Rodríguez-Quintero, J. High Energy Phys. 06 (2008) 099.
[10] V. N. Gribov, Nucl. Phys. **B139**, 1 (1978).

[11] D. Zwanziger, Nucl. Phys. **B209**, 336 (1982).
[12] D. Zwanziger, Nucl. Phys. **B321**, 591 (1989).
[13] D. Zwanziger, Nucl. Phys. **B323**, 513 (1989).
[14] G. Dell'Antonio and D. Zwanziger, Nucl. Phys. **B326**, 333 (1989).
[15] G. Dell'Antonio and D. Zwanziger, Commun. Math. Phys. **138**, 291 (1991).
[16] D. Zwanziger, Nucl. Phys. **B364**, 127 (1991).
[17] D. Zwanziger, Nucl. Phys. **B378**, 525 (1992).
[18] D. Zwanziger, Nucl. Phys. **B399**, 477 (1993).
[19] D. Zwanziger, Nucl. Phys. **B412**, 657 (1994).
[20] D. Zwanziger, Phys. Rev. D **65**, 094039 (2002).
[21] D. Zwanziger, Phys. Rev. D **69**, 016002 (2004).
[22] D. Dudal, S. P. Sorella, N. Vandersickel, and H. Verschelde, Phys. Rev. D **77**, 071501(R) (2008).
[23] D. Dudal, J. A. Gracey, S. P. Sorella, N. Vandersickel, and H. Verschelde, Phys. Rev. D **78**, 065047 (2008).
[24] J. A. Gracey, Phys. Rev. D **82**, 085032 (2010).
[25] G. Curci and R. Ferrari, Nuovo Cimento A **32**, 151 (1976).
[26] G. Curci and R. Ferrari, Nuovo Cimento A **35**, 1 (1976).
[27] G. Curci and R. Ferrari, Nuovo Cimento A **35**, 273 (1976); **47**, 555(E) (1978).
[28] I. Ojima, Z. Phys. C **13**, 173 (1982).
[29] L. Baulieu, Phys. Rep. **129**, 1 (1985).
[30] R. Delbourgo, S. Twisk, and G. Thompson, Int. J. Mod. Phys. A **03**, 435 (1988).
[31] T. Hurth, Helv. Phys. Acta **70**, 406 (1997).
[32] J. de Boer, K. Skenderis, P. van Nieuwenhuizen, and A. Waldron, Phys. Lett. B **367**, 175 (1996).
[33] F. Delduc and S. P. Sorella, Phys. Lett. B **231**, 408 (1989).
[34] A. Blasi and N. Maggiore, Mod. Phys. Lett. A **11**, 1665 (1996).
[35] J. Serreau and M. Tissier, Phys. Lett. B **712**, 97 (2012).
[36] J. Serreau, M. Tissier, and A. Tresmontant, Phys. Rev. D **89**, 125019 (2014).
[37] M. Peláez, M. Tissier, and N. Wschebor, Phys. Rev. D **88**, 125003 (2013).
[38] J. Serreau, M. Tissier, and A. Tresmontant, Phys. Rev. D **92**, 105003 (2015).
[39] M. Tissier, Phys. Lett. B **784**, 146 (2018).
[40] M. Peláez, M. Tissier, and N. Wschebor, Phys. Rev. D **90**, 065031 (2014).
[41] U. Reinosa, J. Serreau, M. Tissier, and N. Wschebor, Phys. Rev. D **96**, 014005 (2017).
[42] J. A. Gracey, M. Peláez, U. Reinosa, and M. Tissier, Phys. Rev. D **100**, 034023 (2019).
[43] F. Gao, S.-X. Qin, C. D. Roberts, and J. Rodriguez-Quintero, Phys. Rev. D **97**, 034010 (2018).
[44] J. Horak, F. Ihssen, J. Papavassiliou, J. M. Pawlowski, and A. Webber, arXiv:2201.09747.
[45] S. Laporta, Int. J. Mod. Phys. A **15**, 5087 (2000).
[46] H. Verschelde, Phys. Lett. B **351**, 242 (1995).
[47] H. Verschelde, S. Schelstraete, and M. Vanderkelen, Z. Phys. C **76**, 161 (1997).
[48] D. Gross and A. Neveu, Phys. Rev. D **10**, 3235 (1974).
[49] P. Forgács, F. Niedermayer, and P. Weisz, Nucl. Phys. **B367**, 123 (1991).
[50] P. Forgács, F. Niedermayer, and P. Weisz, Nucl. Phys. **B367**, 144 (1991).
[51] H. Verschelde, K. Knecht, K. van Acoleyen, and M. Vanderkelen, Phys. Lett. B **516**, 307 (2001).
[52] R. E. Browne and J. A. Gracey, J. High Energy Phys. 11 (2003) 029.
[53] T. Ueda, B. Ruijl, and J. A. M. Vermaseren, Proc. Sci., LL2016 (**2016**) 070.
[54] T. Ueda, B. Ruijl, and J. A. M. Vermaseren, Comput. Phys. Commun. **253**, 107198 (2020).
[55] P. A. Baikov, K. G. Chetyrkin, and J. H. Kühn, Phys. Rev. Lett. **118**, 082002 (2017).
[56] F. Herzog, B. Ruijl, T. Ueda, J. A. M. Vermaseren, and A. Vogt, J. High Energy Phys. 02 (2017) 090.
[57] T. Luthe, A. Maier, P. Marquard, and Y. Schröder, J. High Energy Phys. 10 (2017) 166.
[58] K. G. Chetyrkin, G. Falcioni, F. Herzog, and J. A. M. Vermaseren, J. High Energy Phys. 10 (2017) 179.
[59] R. M. Doria, F. A. B. Rabelo de Carvalho, and S. P. Sorella, Braz. J. Phys. **20**, 316 (1990), https://www.sbfisica.org.br/bjp/download/v20/v20a25.pdf.
[60] J. A. Gracey, Phys. Lett. B **552**, 101 (2003).
[61] D. Dudal, H. Verschelde, and S. P. Sorella, Phys. Lett. B **555**, 126 (2003).
[62] G. 't Hooft, Nucl. Phys. **B190**, 455 (1981).
[63] A. S. Kronfeld, G. Schierholz, and U. J. Wiese, Nucl. Phys. **B293**, 461 (1987).
[64] A. S. Kronfeld, M. L. Laursen, G. Schierholz, and U. J. Wiese, Phys. Lett. B **198**, 516 (1987).
[65] R. E. Browne, D. Dudal, J. A. Gracey, V. E. R. Lemes, M. S. Sarandy, R. F. Sobreiro, S. P. Sorella, and H. Verschelde, J. Phys. A **39**, 7889 (2006).
[66] N. Wschebor, Int. J. Mod. Phys. A **23**, 2961 (2008).
[67] D. Dudal, H. Verschelde, V. E. R. Lemes, M. S. Sarandy, R. F. Sobreiro, S. P. Sorella, M. Picariello, and J. A. Gracey, Phys. Lett. B **569**, 57 (2003).
[68] D. Dudal, H. Verschelde, V. E. R. Lemes, M. S. Sarandy, R. F. Sobreiro, S. P. Sorella, and J. A. Gracey, Phys. Lett. B **574**, 325 (2003).
[69] S. G. Gorishny, S. A. Larin, L. R. Surguladze, and F. K. Tkachov, Comput. Phys. Commun. **55**, 381 (1989).
[70] S. A. Larin, F. V. Tkachov, and J. A. M. Vermaseren, The Form version of Mincer, NIKHEF-H-91-18.
[71] P. Nogueira, J. Comput. Phys. **105**, 279 (1993).
[72] J. A. M. Vermaseren, arXiv:math-ph/0010025.
[73] M. Tentyukov and J. A. M. Vermaseren, Comput. Phys. Commun. **181**, 1419 (2010).
[74] T. van Ritbergen, A. N. Schellekens, and J. A. M. Vermaseren, Int. J. Mod. Phys. A **14**, 41 (1999).
[75] J. A. Gracey, 2022 data, arXiv, https://doi.org/10.48550/arXiv.2207.04940 (2022).
[76] J. M. Chung and B. K. Chung, J. Korean Phys. Soc. **33**, 643 (1998).
[77] K. Knecht and H. Verschelde, Phys. Rev. D **64**, 085006 (2001).
[78] S. P. Martin, Phys. Rev. D **96**, 096005 (2017).
[79] A. von Manteuffel and C. Studerus, arXiv:1201.4330.
[80] Y. Schröder and A. Vuorinen, J. High Energy Phys. 06 (2005) 051.
[81] D. J. Broadhurst, Eur. Phys. J. C **8**, 311 (1999).
[82] A. I. Davydychev and M. Y. Kalmykov, Nucl. Phys. **B605**, 266 (2001).

[83] A. I. Davydychev and M. Y. Kalmykov, Nucl. Phys. **B699**, 3 (2004).
[84] M. Y. Kalmykov, Nucl. Phys. **B718**, 276 (2005).
[85] D. J. Gross and F. J. Wilczek, Phys. Rev. Lett. **30**, 1343 (1973).
[86] H. D. Politzer, Phys. Rev. Lett. **30**, 1346 (1973).
[87] W. E. Caswell, Phys. Rev. Lett. **33**, 244 (1974).
[88] D. R. T. Jones, Nucl. Phys. **B75**, 531 (1974).
[89] O. V. Tarasov, A. A. Vladimirov, and A. Yu. Zharkov, Phys. Lett. **93B**, 429 (1980).
[90] T. van Ritbergen, J. A. M. Vermaseren, and S. A. Larin, Phys. Lett. B **400**, 379 (1997).
[91] Ph. Boucaud, F. De Soto, J. P. Leroy, A. Le Yaouanc, J. Micheli, O. Pène, and J. Rodríguez-Quintero, Phys. Rev. D **79**, 014508 (2009).
[92] B. Blossier, P. Boucaud, F. De soto, V. Morenas, M. Gravina, O. Pène, and J. Rodriguez-Quintero, Phys. Rev. D **82**, 034510 (2010).
[93] J. Beringer *et al.* (Particle Data Group), Phys. Rev. D **86**, 010001 (2012).
[94] I. L. Bogolubsky, E. M. Ilgenfritz, M. Müller-Preussker, and A. Sternbeck, Phys. Lett. B **676**, 69 (2009).
[95] K. I. Kondo, T. Murakami, T. Shinohara, and T. Imai, Phys. Rev. D **65**, 085034 (2002).
[96] M. J. Lavelle and M. Schaden, Phys. Lett. B **208**, 297 (1988).
[97] M. Lavelle and M. Oleszczuk, Mod. Phys. Lett. A **07**, 3617 (1992).
[98] J. Ahlbach, M. Lavelle, M. Schaden, and A. Streibl, Phys. Lett. B **275**, 124 (1992).
[99] Ph. Boucaud, A. Le Yaouanc, J. P. Leroy, J. Micheli, O. Pène, and J. Rodríguez-Quintero, Phys. Rev. D **63**, 114003 (2001).
[100] J. C. Collins and J. A. M. Vermaseren, arXiv:1606.01177.
[101] K. G. Chetyrkin, Nucl. Phys. **B710**, 499 (2005).